N. Jb. Geol. Paläont. Abh. **241** (1) 67–109 Stuttgart, August 2006

Biomagnetostratigraphic analysis of the Gorrondatxe section (Basque Country, Western Pyrenees): Its significance for the definition of the Ypresian/Lutetian boundary stratotype

Gilen Bernaola, Bilbao, **Xabier Orue-Etxebarria,** Bilbao, **Aitor Payros,** Bilbao, **Jaume Dinarès-Turell,** Rome, **Josep Tosquella,** Huelva, **Estibaliz Apellaniz,** Bilbao, **Fernando Caballero,** Bilbao

With 16 figures and 1 table

Bernaola, G., Orue-Etxebarria, X., Payros, A., Dinarès-Turell, J., Tosquella, J., Apellaniz, E. & Caballero, F. (2006): Biomagnetostratigraphic analysis of the Gorrondatxe section (Basque Country, Western Pyrenees): Its significance for the definition of the Ypresian/Lutetian boundary stratotype. – N. Jb. Geol. Paläont. Abh., **241**: 67–109; Stuttgart.

Abstract: The Gorrondatxe beach section is part of a 2300 m thick lower Ypresian – upper Lutetian deep-water marine succession and contains the most extensive Ypresian/Lutetian boundary interval so far reported. The entire 700 m thick uppermost Ypresian-lower Lutetian succession shows a good magnetic signal and is rich in well-preserved calcareous planktonic fossils. Moreover, some of the interbedded turbidites supplied abundant nummulitids, allowing the correlation and calibration of the zonal schemes of larger foraminifers and calcareous plankton. At the Gorrondatxe section, all the events traditionally used to identify the Ypresian/Lutetian boundary occur at different levels, demonstrating that before selecting a section to place the Ypresian/Lutetian boundary stratotype the specific criterion to identify this boundary should be defined. The high-resolution calcareous plankton and larger foraminifer biostratigraphic studies, coupled with the magnetostratigraphic analysis performed in the Gorrondatxe section, show the complete record of events that characterizes the Ypresian/Lutetian boundary interval, highlighting the position of several marker events that are suitable to be selected as the criterion to define the Ypresian/Lutetian boundary. The Gorrondatxe section fulfils most of the requirements demanded of a Global Stratotype Section and Point (GSSP) by the International Commission on Stratigraphy, and consequently it is proposed here as a candidate for the GSSP of the base of the Lutetian.

0077-7749/06/0241-0067 $ 10.75

Zusammenfassung: Das Gorrondatxe-Strandprofil ist Teil einer 2300 m mächtigen Abfolge von tiefmarinen Ablagerungen, die vom unteren Ypresium bis ins obere Lutetium reichen. Dieses Profil enthält den mächtigsten bis jetzt beschriebenen Grenzbereich der Ypresium/Lutetium-Grenze. Die gesamte 700 m mächtige Abfolge, die dem obersten Ypresium und dem untersten Lutetium entspricht, weist gute magnetische Signale auf und ist reich an gut erhaltenen kalkschaligen planktonischen Fossilien. Die zahlreichen Nummulitiden in den eingeschaltenen Turbiditen ermöglichen die Korrelation und Kalibrierung der auf Großforaminiferen und kalkigem Plankton beruhenden Zonierungen. Alle Kriterien, die traditionell für die Festlegung der Ypresium/Lutetium-Grenze gebraucht worden sind, finden sich im Gorrondatxe-Profil in unterschiedlichen Horizonten. Es ist daher unumgänglich, dass zuerst das Kriterium für diese Grenze bestimmt wird, bevor der entsprechende Grenz-Stratotyp festgelegt wird. Die im Gorrondatxe-Profil in Kombination mit der magnetostratigraphischen Analyse durchgeführten hochauflösenden biostratigraphischen Untersuchungen am kalkschaligen Plankton und den Großforaminiferen zeigen ein vollständiges Register der Ereignisse, welche das Interval der Ypresium/Lutetium-Grenze charakterisieren. Hervorgehoben werden diejenigen Ereignisse, die als gutes Kriterium für die Festlegung dieser Grenze in Frage kommen. Das Gorrondatxe-Profil erfüllt eine Vielzahl der von der Internationalen Stratigraphischen Kommission an einen "Global Stratotype Section and Point" (GSSP) gestellten Ansprüche und wird daher als Kandidat für den GSSP die Untergrenze des Lutetium und damit der Ypresium/Lutetium-Grenze vorgeschlagen.

Keywords: Ypresian/Lutetian boundary, GSSP, Eocene, calcareous nannofossils, planktonic foraminifera, nummulitids, magnetostratigraphy, Gorrondatxe, Pyrenees.

1. Introduction

During the 28th International Geological Congress held in Washington D.C. in 1989, the International Subcomission on Paleogene Stratigraphy (ISPS) agreed on a set of Paleogene stages. Subsequently, official Working Groups and Regional Committees were set up to find a Global Stratotype Section and Point (GSSP) for the lower boundary of each of these Stages. At present, all the GSSPs of the Paleogene epochs (i.e., base of Paleocene = base of Danian; base of Eocene = base of Ypresian; base of Oligocene = base of Rupelian; and top of Oligocene = base of Aquitanian) have been established and ratified by the International Union of Geological Sciences. The search for the remaining Paleogene GSSPs (i.e., base of Selandian, Thanetian, Lutetian, Bartonian, Priabonian and Chattian) is still in progress, and it is hoped to present all the proposals prior to the next International Geological Congress in 2008.

According to the International Commission on Stratigraphy (ICS) guidelines, clearly summarized by REMANE et al. (1996), a prospective stratotype section should contain the best possible record of the relevant marker events and, in addition, should fulfil as many of the following requirements as possible:

(1) Geological requirements: exposure over an adequate thickness of sediments; continuous sedimentation; high rate of sedimentation; absence of synsedimentary and tectonic disturbances; absence of metamorphism and strong diagenetic alteration; potential for radioisotopic dating, magnetostratigraphy and chemostratigraphy; knowledge of the regional paleogeographic and sequence stratigraphic context.

(2) Biostratigraphic requirements: abundance and diversity of well preserved fossils; absence of vertical facies changes at or near the boundary; favourable facies for long-range biostratigraphic correlations (open marine deposits).

(3) Infrastructure requirements: accessibility; free access; possibility to fix a permanent marker; permanent protection of the site.

The aim of this paper is to present new bio- and magnetostratigraphic data of the Ypresian/Lutetian (Early/Middle Eocene) boundary transition at the Gorrondatxe section (Basque Country, western Pyrenees), and to propose this section as a candidate to locate the GSSP of the base of the Lutetian Stage (i.e., Ypresian/Lutetian boundary), as this section fulfils most of the requirements listed above.

Originally, the Lutetian was defined by DE LAPPARENT (1883) to refer to the socalled "Calcaire Grossier" of the Paris Basin. Later, BLONDEAU et al. (1980) proposed two neostratotypes 50 km North of Paris, namely the Saint-Leu d'Esserent and Saint-Vaast-Les-Mellos sections. However, the Lutetian sections around Paris, and even elsewhere in northern Europe, are not suitable candidates to be designated as the GSSP since they display shallow-marine deposits and/or the base of those sections corresponds to a regional unconformity (e.g., AUBRY 1986, 1995; STEURBAUT 1988).

The lower part of the Lutetian "Calcaire Grossier" is best typified by the occurrence of abundant specimens of *Nummulites laevigatus*, a species whose range coincides with Zone SBZ13 of SERRA-KIEL et al. (1998). In addition, AUBRY (1986) demonstrated that, in terms of calcareous nannofossils, the base of the "Calcaire Grossier" pertains to the Subzone CP12b of OKADA & BUKRY (1980). AUBRY et al. (1986) carried out the correlation of the Lutetian strata in Paris with those of the Hampshire-London basin based on calcareous nannofossil and *Nummulites* faunas. There, they integrated

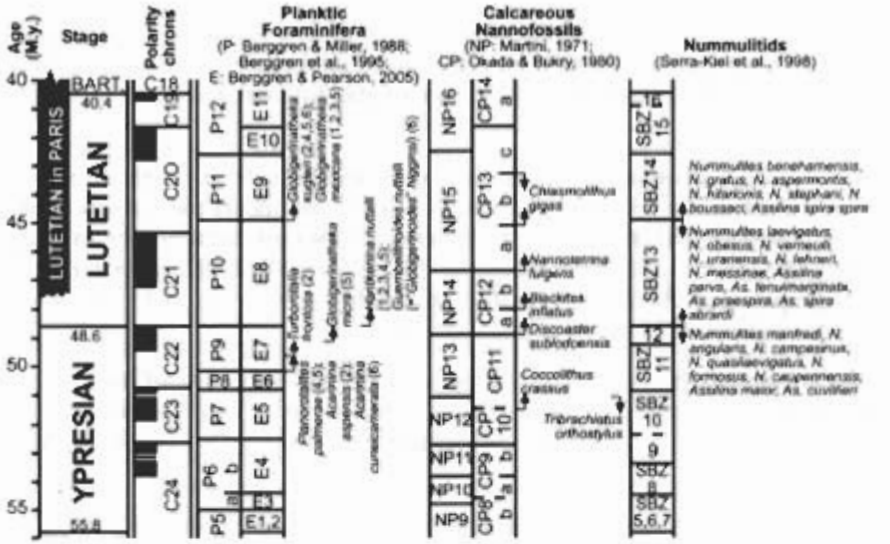

Fig. 1. Ypresian – Lutetian standard biomagnetochronostratigraphic framework. The extent of the Lutetian strata in Paris is shown for comparison purposes. Absolute ages are from LUTERBACHER et al. (2004). Correlation between magnetic polarity chrons, planktonic foraminiferal zones, and calcareous nannofossil zones is from BERGGREN et al. (1995) and BERGGREN & PEARSON (2005). Planktonic foraminiferal events are as follow: (1) STAINFORTH et al. 1975; (2) BLOW 1979; (3) TOUMARKINE & LUTERBACHER 1985); (4) BERGGREN et al. 1995; (5) PREMOLI SILVA et al. (2003); (6) BERGGREN & PEARSON (2005); correlation of events by (1), (2) and (3) with magnetic polarity chrons is based on BERGGREN & MILLER (1988).

biostratigraphic and magnetostratigraphic data and proposed that the Lutetian strata correspond to magnetic polarity chron C21.

Although planktonic foraminifera are rare in these North European sections, the criterion most commonly used during the last half century to place the base of the Lutetian has been the first appearance of specimens belonging to the planktonic foraminiferal genus *Hantkenina,* which also

marks the base of Zone P10 of BERGGREN et al. (1995). Unfortunately, Eocene hantkeninids are restricted to lower and middle latitudes. In addition, they are not abundant at their inception and seldom reached high percentages in well preserved Eocene faunas (PREMOLI SILVA & BOERSMA 1988: 323; COXALL et al. 2003: 237). Consequently, different planktonic foraminifer events have commonly been taken as approximate markers of the base of Zone P10 and, hence, of the Lutetian Stage (e.g., ORUE-ETXEBARRIA & APELLANIZ 1985; ERBACHER et al. 2004; ZACHOS et al. 2004; PAYROS et al. 2006). In this respect, BERGGREN & PEARSON (2005) indicated that the first appearance of *Guembelitrioides nuttalli* (= "*Globigerinoides*" *higginsi*, which marks the base of their Zone E8, equivalent to Zone P10 of BERGGREN et al. 1995) occurs at a level close to the first appearance of hantkeninids and, therefore, that it can be used to denote the base of the Middle Eocene. The correlation between magnetostratigraphic and different biostratigraphic scales has improved over time (e.g., BERGGREN 1972; HARDENBOL & BERGGREN 1978; BERGGREN & MILLER 1988; BERGGREN et al. 1995; LUTERBACHER et al. 2004), and today it is considered that the first appearances of the first specimens of the genus *Hantkenina* and of the taxon *Guembelitrioides nuttalli* coincide with the boundary between the magnetozones C22n and C21r (BERGGREN et al. 1995; BERGGREN & PEARSON 2005). Fig. 1 summarizes the currently most accepted biomagnetochronostratigraphic correlation scheme for the Ypresian/Lutetian boundary interval.

In the light of the geological, biostratigraphic and infrastructure requirements specified by the ICS for any prospective GSSP and the different criteria used so far to define the base of the Lutetian Stage, the study of the Gorrondatxe section was undertaken from the viewpoint of the general stratigraphic context (paleogeography, lithostratigraphy and sequence stratigraphy), calcareous nannofossil biostratigraphy, planktonic foraminiferal biostratigraphy, nummulitid biostratigraphy and magnetostratigraphy.

2. Geological Setting

The Gorrondatxe section is exposed on the cliffs of an easily accessible beach (also known as Azkorri section because of the cape on the northeastern side of the beach) just northwest of Bilbao (Latitude: 43°23'N; Longitude: 3°01'50"W; Figs. 2 and 3). The beach, awarded the European Union Blue Flag for water cleanliness and beach services, is equipped with a car park, fountains, bars and bus services (further details at http://www.bizkaia.net/ingurugiroa_Lurraldea/Hondartzak/in_home3.htm).

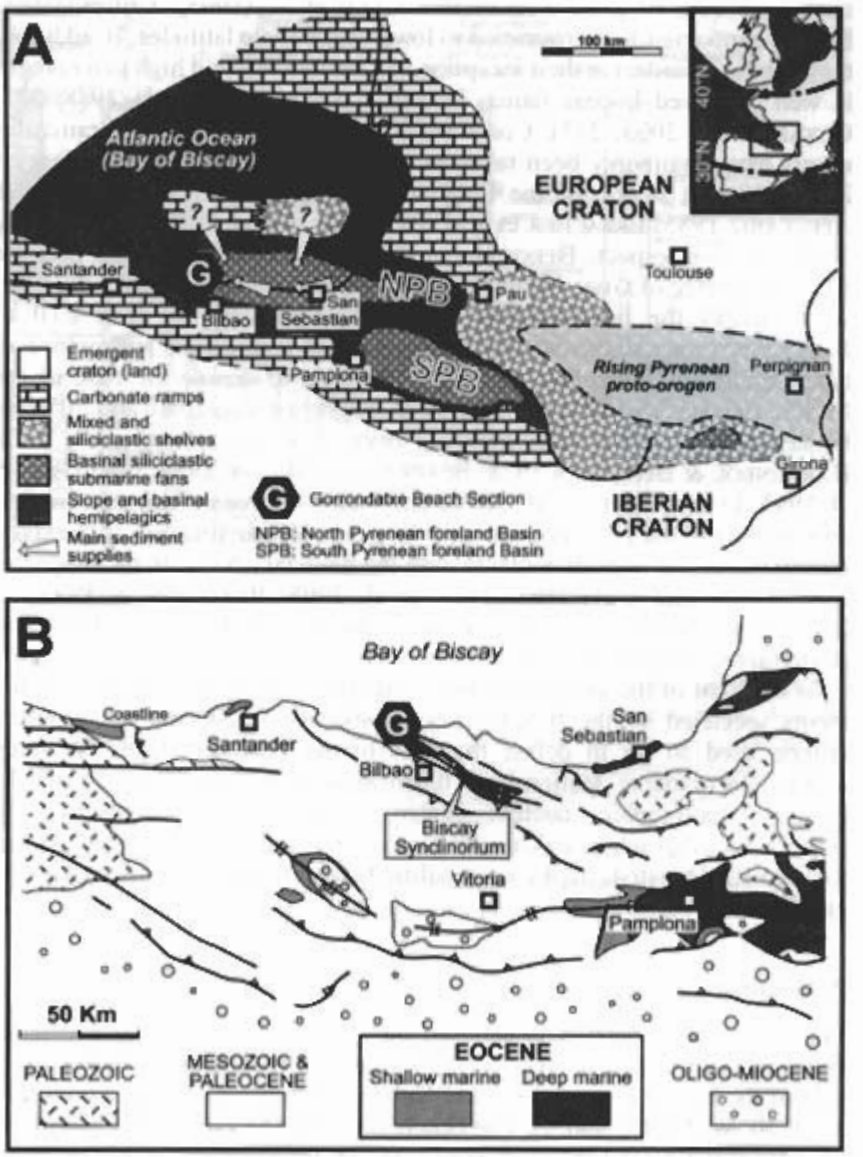

Fig. 2 (Legend see p. 73)

3. Paleogeography

During Eocene times, the area studied formed part of a narrow marine gulf created by the oblique convergence of the Iberian and European plates (Fig. 2A). The gulf, located at approximately -35°N latitude, opened northwest into the Bay of Biscay and had shallow carbonate ramps on its northern and southern margins (PLAZIAT 1981; PUJALTE et al. 2002). Further plate convergence during Eocene times caused the tectonic uplift of the Pyrenees, and two foreland basins developed to the south and north of the rising orogen (Fig. 2A; VERGES et al. 1995; PAYROS 1997; PUJALTE et al. 2002).

Today, deep marine deposits are extensively exposed in the coastal provinces of the Basque Country, whereas remains of the southern shallow-water carbonate ramp are found in the southern provinces (Fig. 2B). The present study focuses on the western, most distal part of the northern foreland basin. This area received sediments from several sources, notably hemipelagic marls and limestones, calciclastic turbidites and debrites thought to be derived from northern sources, and siliciclastic turbidites coming from northern and eastern sources (Fig. 2A) (PAYROS et al. 2006). Estimated palaeodepth for this area is about 1500 m (ORUE-ETXEBARRIA & LAMOLDA 1985; RODRÍGUEZ-LÁZARO & GARCÍA-ZARRAGA 1996; PAYROS et al. 2006).

4. Lithostratigraphy

The Gorrondatxe section is part of a 2300 m thick lower Ypresian-upper Lutetian succession that extends from the town of Sopela to the Galea Cape and is exposed in coastal cliffs (Fig. 3). It is entirely composed of deep-marine deposits, which were uplifted and tilted during the Alpine Orogeny and are now part of the northeastern limb of the Biscay Synclinorium. The succession, despite being almost continuous, is affected by several faults, one of which divides the lower part of the Gorrondatxe section into two separate parts (Fig. 3).

The Sopela-Galea section has earlier been the subject of detailed sedimentological (PUJALTE et al. 1997) and micropaleontological analyses

Fig. 2. (A) Early Paleogene paleogeography of the Pyrenean area without palinspastic restoration (party based on PLAZIAT 1981, PUJALTE et al. 2002, and our own data). (B) Simplified geological map of the Western Pyrenees showing the most important Eocene outcrops. The location of the Gorrondatxe section (G) is shown on both maps.

(Orue-Etxebarria et al. 1984; Orue-Etxebarria 1985; Orue-Etxebarria & Lamolda 1985; Rodríguez-Lázaro & García-Zarraga 1996), one of which dealt specifically with the Ypresian/Lutetian boundary in the Gorrondatxe beach section (Orue-Etxebarria & Apellaniz 1985). However, only general stratigraphic descriptions of it have so far been produced (e.g. Rat 1959; Payros et al. 2006) and no formal lithostratigraphic units have yet been defined (Fig. 3). According to these descriptions, the lower half of the succession is composed of hemipelagic marls interspersed with siliciclastic turbidites, which peak in abundance in the so-called Azkorri Sandstone (Rat 1959). Resedimented carbonate deposits become progressively more abundant in the upper half of the succession.

The Gorrondatxe beach section, 700 m thick, extends from the top of the Azkorri Sandstones to the base of the calciturbiditic flysch (Fig. 3). It is mostly composed of hemipelagic marls and limestones, but thin-bedded (<10 cm) siliciclastic turbidites are also common. In addition, some thick-bedded (10-240 cm) mixed turbidites (siliciclastic and carbonate) occur at some levels of the succession.

5. Sequence stratigraphy

Sequence stratigraphic units (e.g., third order depositional sequences) are the result of eustatic or relative changes in sea level, which result in characteristic stratal architectures (e.g., Vail et al. 1991). According to current sequence stratigraphic models, basinal lowstand deposits are best typified by turbidite accumulations, whereas basinal transgressive and highstand deposits are mostly hemipelagic.

Payros et al. (2006) investigated the sedimentary features (lithology, thickness and shape, primary structures, grain fabric, palaeocurrents, etc.) of every turbidite bed thicker than 15 cm in order to assess volumetric variations of turbidites throughout the Sopela-Galea section (Fig. 3). They

Fig. 3. (A) Simplified geological map of the study area, showing the location of the Gorrondatxe beach section. (B) Simplified litholog of the Sopela-Galea succession, showing the extent of the Gorrondatxe beach section. Planktonic foraminifera biostratigraphy (left-hand column) is from Orue-Etxebarria et al. (1984); informal lithostratigraphic units are mostly based on Rat (1959); vertical variations in turbidite content (right-hand graph) are from Payros et al. (2006); depositional sequences are those defined by Payros (1997) and Pujalte et al. (2000) in the Pamplona area.

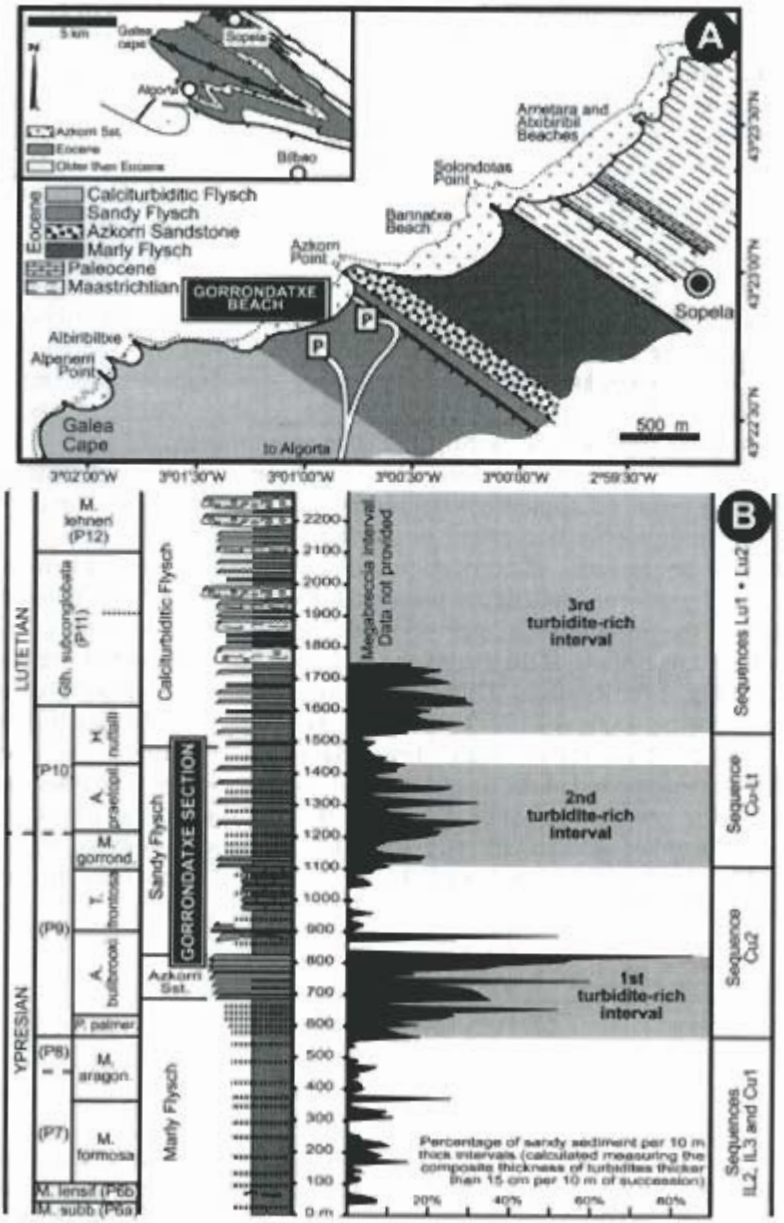

Fig. 3 (Legend see p. 74)

obtained a semiquantitative estimation of the vertical variations in turbidite abundance by plotting their composite thickness in 10 m thick intervals. This procedure made evident that the Sopela-Galea succession consists of six distinct intervals with variable amounts of turbidites. The turbidite content of three intervals rarely exceeds 20 %, average values being lower than 10 % and some levels almost completely devoid of turbidites. These three intervals were called consequently "turbidite-poor". On the other hand, the other three intervals were named "turbidite-rich" because their turbidite content ranges from 10 % to 80 %, the average being more than 20 %. PAYROS et al. (2006) also noted an increase in the proportion of carbonized plant remains and reworked shallow-water benthic faunas in the three turbidite-rich intervals.

However, the sequence stratigraphic interpretation of the Sopela-Galea section is not straightforward, since sequence stratigraphic units defined solely on the basis of 1D profiles are not reliable. Unfortunately, the platform areas from which the Sopela-Galea resedimented deposits derived have eroded away and, therefore, the significance of the turbidite-rich intervals in terms of sequence stratigraphy cannot be verified. Hence, the sequence stratigraphic framework of the Sopela-Galea section can only be established on the basis of correlation with neighbouring areas where both basinal and platform deposits are preserved. PAYROS et al. (2006) noted that the ages of the turbidite-rich intervals correlate precisely with those of resedimented basinal units of the Pamplona area, 200 km southeast of the study area (see Fig. 2 for location). There, based on the study of deep and shallow-water deposits, PAYROS (1997) and PUJALTE et al. (2000) distinguished twelve third-order lower Ypresian – lower Bartonian depositional sequences, which were interpreted as the result of tectonically induced regional sea-level changes. The lowstand turbiditic deposits of their fourth (Cu-2), fifth (Cu-Lt) and sixth together with seventh (Lu-1 + Lu-2) sequences correlate with the turbidite-rich intervals of the Sopela-Galea succession, supporting the interpretation of the latter as regional lowstand deposits (Fig. 3).

Fig. 4. Selected calcareous nannofossil species ranges and location of the main biohorizons across the Ypresian/Lutetian transition at the Gorrondatxe section. Broken lines indicate very rare occurrences. Zones in column (a) are following OKADA & BUKRY (1980); those in column (b) are following MARTINI (1971).

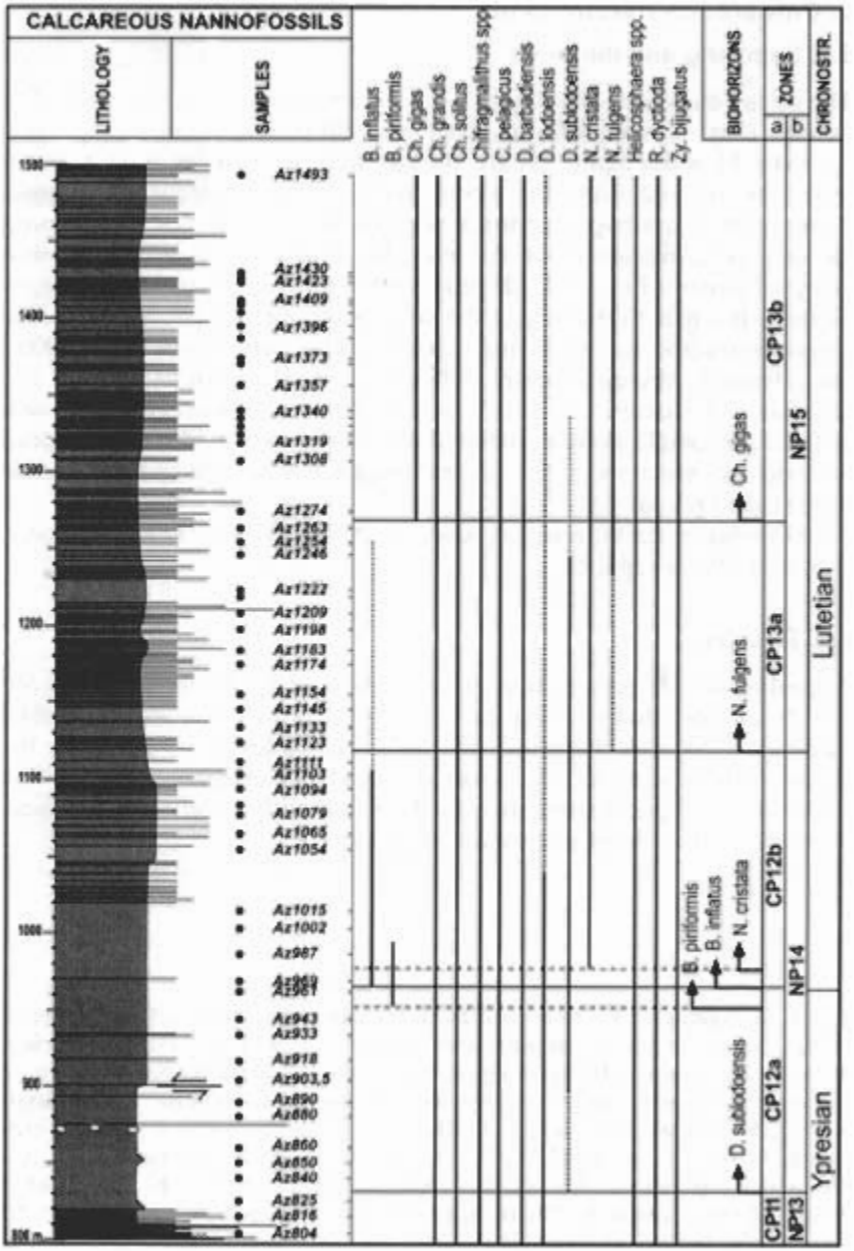

Fig. 4 (Legend see p. 76)

6. Calcareous nannofossils

6.1. Sampling and methods

The calcareous nannofossil study is based on the analysis of a total of 56 samples (Fig. 4). Samples were taken every 20 m with closer intervals near the main biostratigraphic events. Smear slides of samples were prepared from raw material using the pipette method for calcareous nannofossils (Bown 1998), avoiding mechanical or physical processes that could modify the original composition of the assemblage. All the smear slides were analyzed under a Leica DMLP petrographic microscope at 1500X magnification. In order to investigate the smallest species, to observe details of bigger forms and to take pictures, smear-slides were examined at 2000X magnification. Microphotographs of significant calcareous nannofossil taxa are shown in Figures 5, 6 and 7. At least 300 nannofossil specimens were counted per sample along a random traverse on the slide. Moreover, in order to detect rare species with key biostratigraphic value, three additional tracks were studied per sample.

In this paper, the biozonation schemes of Martini (1971) and Okada & Bukry (1980) are applied.

6.2. Results

According to the preservation criteria proposed by Roth & Thierstein (1972) all the studied samples from the Gorrondatxe section yielded moderately to well-preserved calcareous nannofossil assemblages that occasionally show traces of dissolution and in lesser extent re-crystallization. Preservation of calcareous nannofossils is frequently excellent and delicate structures and coccospheres are usually present.

Fig. 5. All figures are from Gorrondatxe section and were taken with parallel nicols except (a), which was taken with cross-polarized light. The scale bar represents 10 μm in all figures. **a-b**) *Chiphragmalithus calathus*, sample Az903; **c**) *Chiphragmalithus acanthodes*, sample Az969, **d-k**) *Nannotetrina cristata*, d-e – sample Az987, f – lateral view, sample Az1002, g – sample Az1015, h – lateral view, sample Az1079, i – sample Az1103, j. – sample Az1209, k – sample Az1246; **l, o**) *Discoaster sublodoensis*, l – sample Az943, o – sample Az903; **p**) *Discoaster* cf. *D. sublodoensis*, sample Az890; **m, n, q**) *Nannotetrina fulgens*, m – sample Az1209, n – sample Az1246, q – sample Az1154; **r-s**) *Discoaster lodoensis*, r – sample Az969, s – sample Az890.

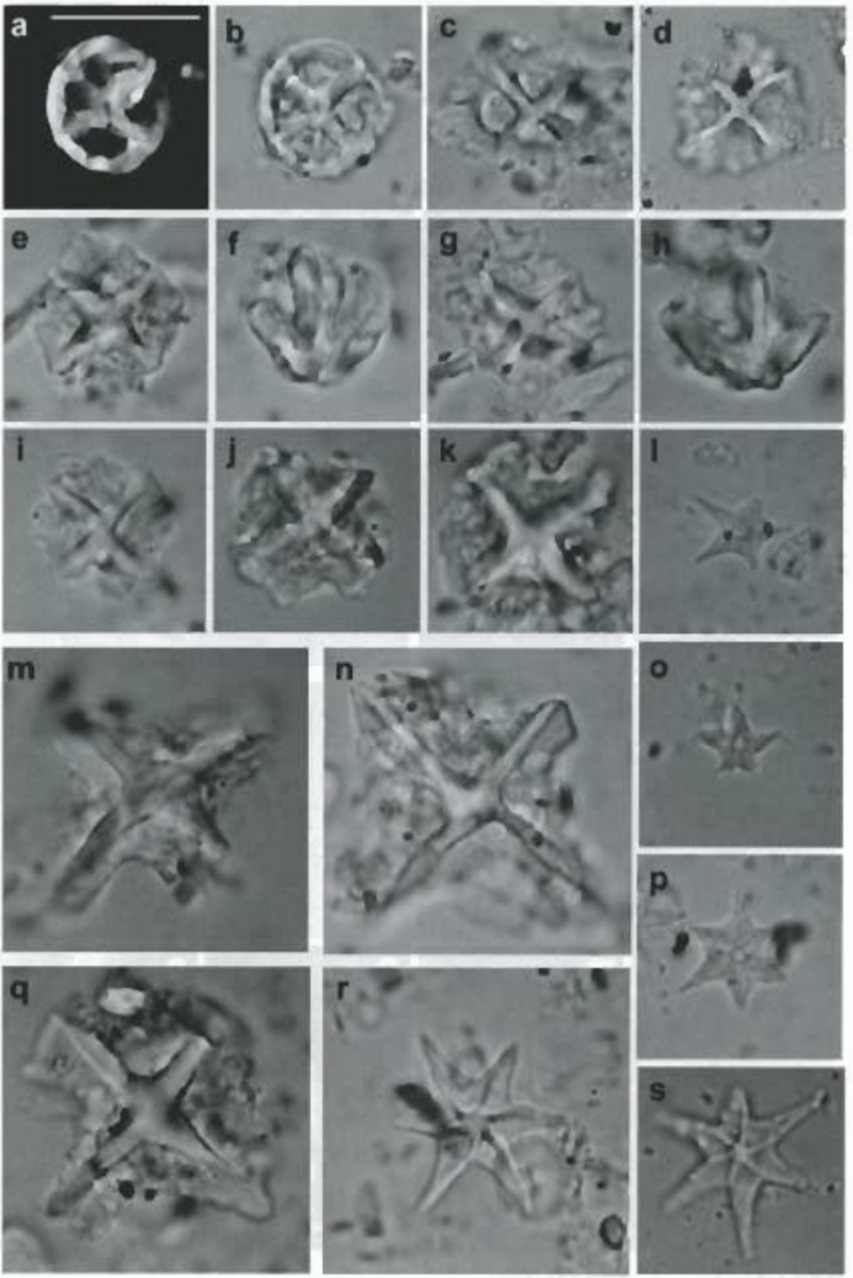

Fig. 5 (Legend see p. 78)

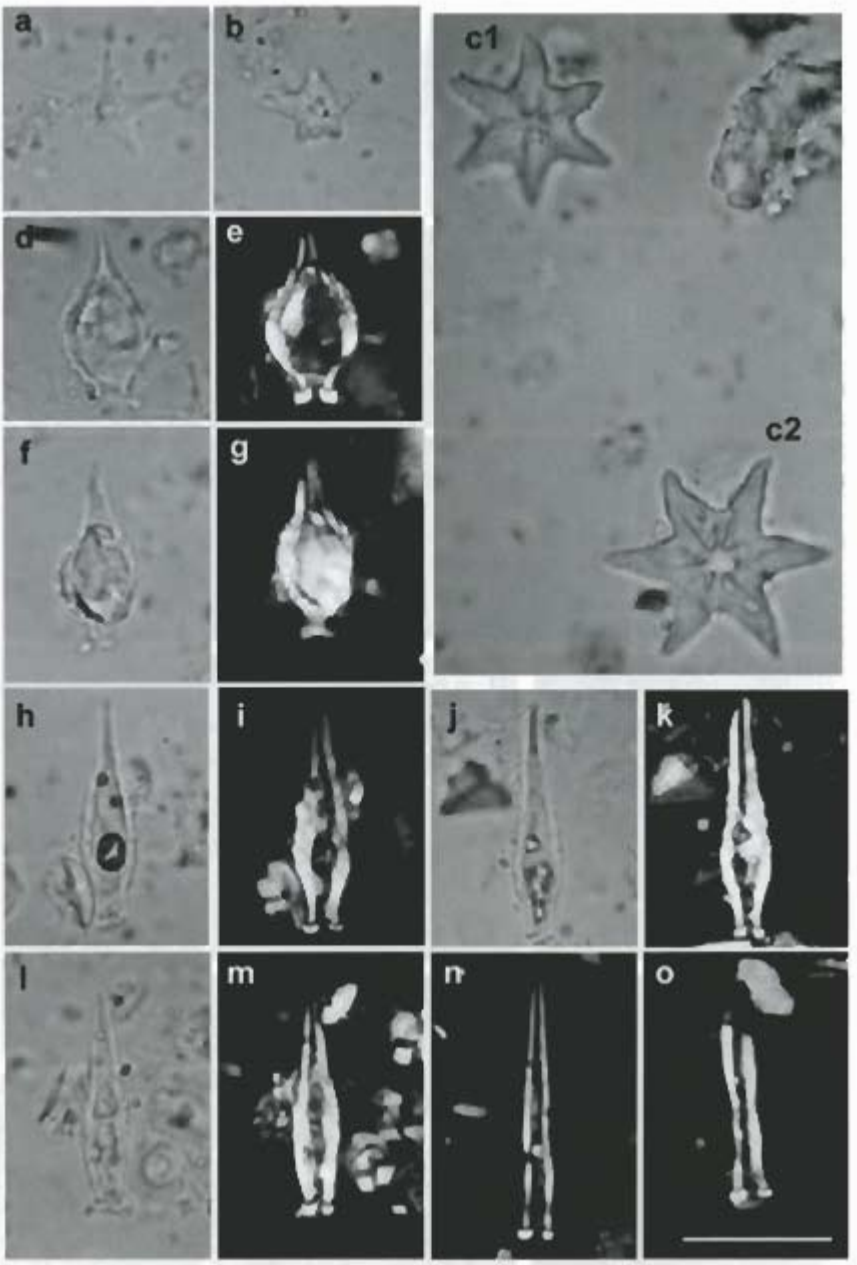

Fig. 6 (Legend see p. 81)

The high diversity and total abundance of calcareous nannofossils are remarkably regular throughout the succession with an average of 45 species per sample and 17 specimens per field of view.

The assemblages are dominated by common to abundant *Reticulofenestra* and *Coccolithus*, with less common *Ericsonia*, *Sphenolithus*, *Zygrhablithus* and *Chiasmolithus*, the latter increasing upsection in abundance and size.

Reworked nannofossils occur in all the samples. Most of them are of Cretaceous and in lesser quantity Paleocene and early Eocene age. The reworking results from the nature of the sediments, limestone-marlstone alternations with a high number of interbedded turbidites. The presence of reworked nannofossils can occasionally obscure the location of the latest occurrence (LO) of some taxa. Taking into account that the reworking is not very intense and is not equally present throughout the succession, the LO of a species was tentatively located at the end of its continuous occurrence. In this work, however, in order to minimize the possible error of considering the top of the continuous occurrence of a species as its latest occurrence, we only use the first occurrence (FO) of selected species.

The studied interval spans from the upper part of the Zone CP11 to the Subzone CP13b.

The summary of recognized zones and main biohorizons is given in Fig. 4 and described in detail below:

a) FO of *Discoaster sublodoensis* (CP11/CP12a; NP13/NP14): At the Gorrondatxe section the FO of *D. sublodoensis* has been recorded in sample Az840, 40 m above the base of the studied succession. From sample Az840 to Az890 this taxon is rare to very rare and its preservation is usually poor. In this 50-m-thick interval, transitional forms between *Discoaster lodoensis* and *D. sublodoensis* have also been found. These forms are six-rayed *Discoaster* with straight or only slightly curved arms (Fig. 5p). From sample Az903.5 upward, the presence of *D. sublodoensis* is more common and the

Fig. 6. All figures are from Gorrondatxe section and were taken with parallel nicols except (e), (g), (i), (k), (m-o), which were taken with cross-polarised light. The scale bar represents 10 μm in all figures. **a-b)** *Discoaster sublodoensis*, sample Az840; **c1-2)** *Discoaster lodoensis*, sample Az840; **d-g)** *Blackites piriformis*, d-e – sample Az969, f-g – sample Az961; **h-m)** *Blackites inflatus*, h-i – sample Az987, j-k – sample Az1002, l-m – sample Az969; **n)** *Blackites spinosus*, sample Az943; **o)** *Blackites* cf. *B. perlongus*, sample Az943.

specimens are better preserved (Figs. 5l, 5o). A similar abundance trend was also observed in the Possagno section, Southern Alps (AGNINI et al. 2006). This confirms that *D. sublodoensis* is usually rare in its lower range in many sections (ROMEIN 1979; VAROL 1989).

b) FO of *Blackites piriformis*: The FO of *B. piriformis* precedes the FO of *Blackites inflatus*, the CP12b marker. These two taxa could be confused in poorly preserved material, especially in those samples where recrystallization is strong. At the Gorrondatxe section, the range of *B. piriformis* is very short. It first appears in sample Az961 and disappears 26 m higher, in sample Az987. This species is also rare and sporadic in other well-preserved successions (BOWN 2005).

c) FO of *Blackites inflatus* (CP12a/CP12b): As mentioned above, this species is prone to dissolution/recrystallization in poorly preserved material and is usually absent or very rare. In fact, the first appearance datum (FAD) of *B. inflatus* is one of the worst documented datums of the Ypresian/Lutetian boundary time interval (BERGGREN et al. 1995). We found its FO at sample Az969, 129 meters above the base of Zone CP12a.

d) FO of *Nannotetrina* spp.: This biohorizon is usually used to define the base of CP13 in sections where the presence of *Nannotetrina fulgens* is very rare or absent (PERCH-NIELSEN 1985). However, we advise against the use of this biohorizon to mark the base of Zone CP13 as we actually found the FO of *Nannotetrina* spp., *N. cristata*, in sample Az987, in the lower part of Subzone CP12b. Other biohorizons, such as the LO of *B. inflatus* (AUBRY 1983; VAROL 1989) or the LO of *D. sublodoensis* (LYLE et al. 2002), have occasionally been used to approximate the base of CP13 Zone.

e) FO of *Nannotetrina fulgens* (CP12b/CP13a; NP14/NP15): In the Gorrondatxe section the FO of *N. fulgens* is recorded in sample Az1111,

Fig. 7. All figures are from Gorrondatxe section and were taken with cross-polarised light except (b), (f), (i), (j) and (m), which were taken with parallel nicols. The scale bar represents 10 µm in all figures. **a-b)** *Coccolithus staurion* [= *C. mutatus* (PERCH-NIELSEN 1971) BOWN 2005], sample Az1409; **c-d)** *Campilosphaera dela*, sample Az943; **e-f)** *Chiasmolithus grandis*, sample Az1319; **g, j)** *Chiasmolithus solitus*, sample Az943; **h-i, l-m)**, *Chiasmolithus gigas*, h-i – sample Az1495, l-m – sample Az1396; **k, n)** *Reticulofenestra dictyoda*, k – sample Az943, n – small form, sample Az943.

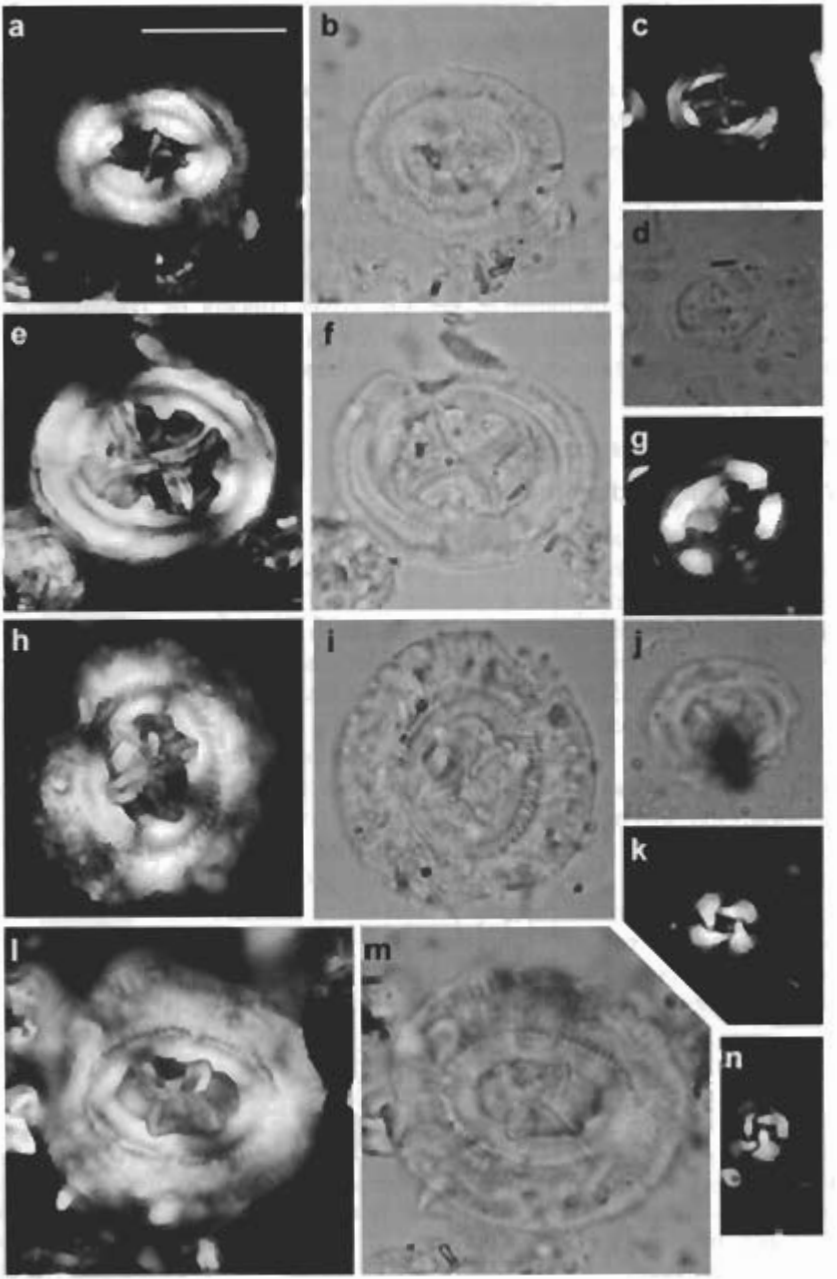

Fig. 7 (Legend see p. 82)

271 m above the base of CP12. This taxon is rare in the lower part of its range, but increases in abundance from sample Az1246 upwards.

f) FO of *Chiasmolithus gigas* (CP13a/CP13b): This biohorizon, marked by the first *Chiasmolithus* larger than 19 μm with a broad distal shield and restricted central opening spanned by a relatively small x-shaped structure with sigmoid bars, is located at sample Az1274. We do not include in *Ch. gigas* the forms that BOWN (2005) redefined as *Coccolithus mutatus* (PERCH-NIELSEN 1971) BOWN 2005. According to this author those forms (very large coccoliths with wide central-area and narrow, axial to slightly rotated cross-bars) are probably included in the *Ch. gigas* concept of BRAMLETTE & SULLIVAN (1961). The last occurrence of *Ch. gigas* has not been detected, its presence being continuous up to the top of the studied interval.

7. Planktonic foraminifera

7.1. Sampling and methods

To analyze the planktonic foraminifera of the Gorrondatxe section, 96 samples (each of about 1 kg) were collected, which were very close-spaced near the main biostratigraphic events (Fig. 8). The samples were washed and screened to obtain residues of a 100-630 μm size range, which were studied under a binocular microscope. The complete assemblage of planktonic foraminifers was recorded to species level. For taxonomic purposes significant species were imaged with a JEOL Scanning Electron Microscope, model JSM-6400 (Figs. 9 and 10). After a separation with an Otto microspliter, relative abundances of the different species were estimated based on counts of about 300 specimens. All residues contained planktonic foraminifers in sufficient quantity and degree of preservation to permit a semiquantitative study designed to determine the FO and LO of planktonic foraminifer species. On the basis of these data, and taking into account the great thickness of the Gorrondatxe succession, a new high-resolution planktonic foraminiferal biozonation is proposed for the studied interval, although the standard tropical-subtropical zonation schemes of BERGGREN et al. (1995)

Fig. 8. Selected planktonic foraminifer species ranges and location of the main biohorizons across the Ypresian/Lutetian transition at the Gorrondatxe section. Biozones in column (a) are as described in this study; those in column (b) are following BERGGREN et al. (1995) (P scale) and BERGGREN & PEARSON (2005) (E scale).

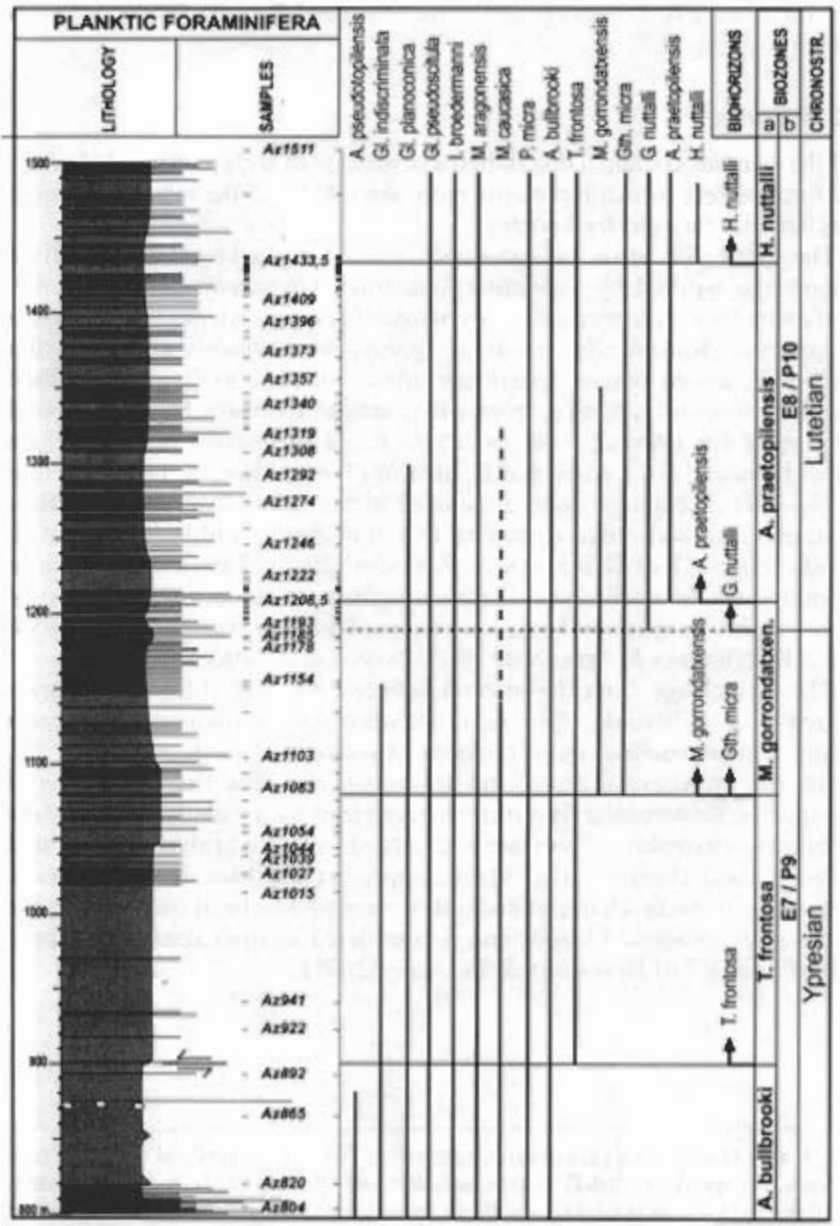

Fig. 8 (Legend see p. 84)

and BERGGREN & PEARSON (2005) are also used for correlation purposes (Fig. 8).

7.2. Results

All the samples contain a diversified assemblage of well-preserved planktonic foraminifers, which represents more than 90 % of the total (planktonic plus benthic) foraminiferal content.

The lower 100 m of the succession present a planktonic foraminiferal assemblage typified by *Subbotina linaperta*, *"Guembelitrioides" lozanoi*, *Globanomalina planoconica*, *Pseudohastigerina micra*, *Morozovella aragonensis*, *Morozovella caucasica*, *Igorina broedermanni* and *Acarinina bullbrooki*, among others. Specimens similar in shape to *G. nuttalli*, albeit smaller in size and lacking supplementary sutural apertures, have been found throughout this interval; these specimens might correspond to intermediate forms between *"G." lozanoi* and *G. nuttalli* (TOUMARKINE & LUTERBACHER 1985). This assemblage is here included in the *Acarinina bullbrooki* Biozone, and is considered as equivalent to part of Zone P9 of BERGGREN et al. (1995), Zone E7 of BERGGREN & PEARSON (2005). This interpretation is supported by the occurrence of *Planorotalites palmerae*, marker taxon of Zone P9, 250 m lower in the succession (see ORUE-ETXEBARRIA et al. 1984; ORUE-ETXEBARRIA & APELLANIZ 1985; PAYROS et al., 2006).

The assemblage from the interval between 900 and 1083 m is characterized by *A. bullbrooki*, *P. micra*, *I. broedermanni*, *S. linaperta*, *Subbotina senni*, *Globanomalina indiscriminata*, *Globanomalina planoconica*, *M. caucasica*, *Morozovella crater* and *M. aragonensis*. The first specimens of the species *Turborotalia frontosa*, characterized by a rather high arch-like umbilical-extraumbilical aperture with a faint lip and a fairly well separated globular final chamber (Fig. 9j-m), appear at the base of this interval. According to these characteristics, this interval has been included in the *Turborotalia frontosa* Biozone and is considered as equivalent to the upper part of Zone E7 of BERGGREN & PEARSON (2005).

Fig. 9. a-c) *Morozovella caucasica* (GLAESSNER, 1937), a – umbilical view, b – lateral view, c – spiral view; **d-f)** *Acarinina bullbrooki* (BOLLI, 1957), d, f – spiral view, e – umbilical view; **g-i)** *Globigerinatheka micra* (SHUTSKAYA, 1958), g, h – umbilical view, i – spiral view; **j-m)** *Turborotalia frontosa* (SUBBOTINA, 1953), j – spiral view, k – lateral view, l, m – umbilical view. Scale bar = 100 μm.

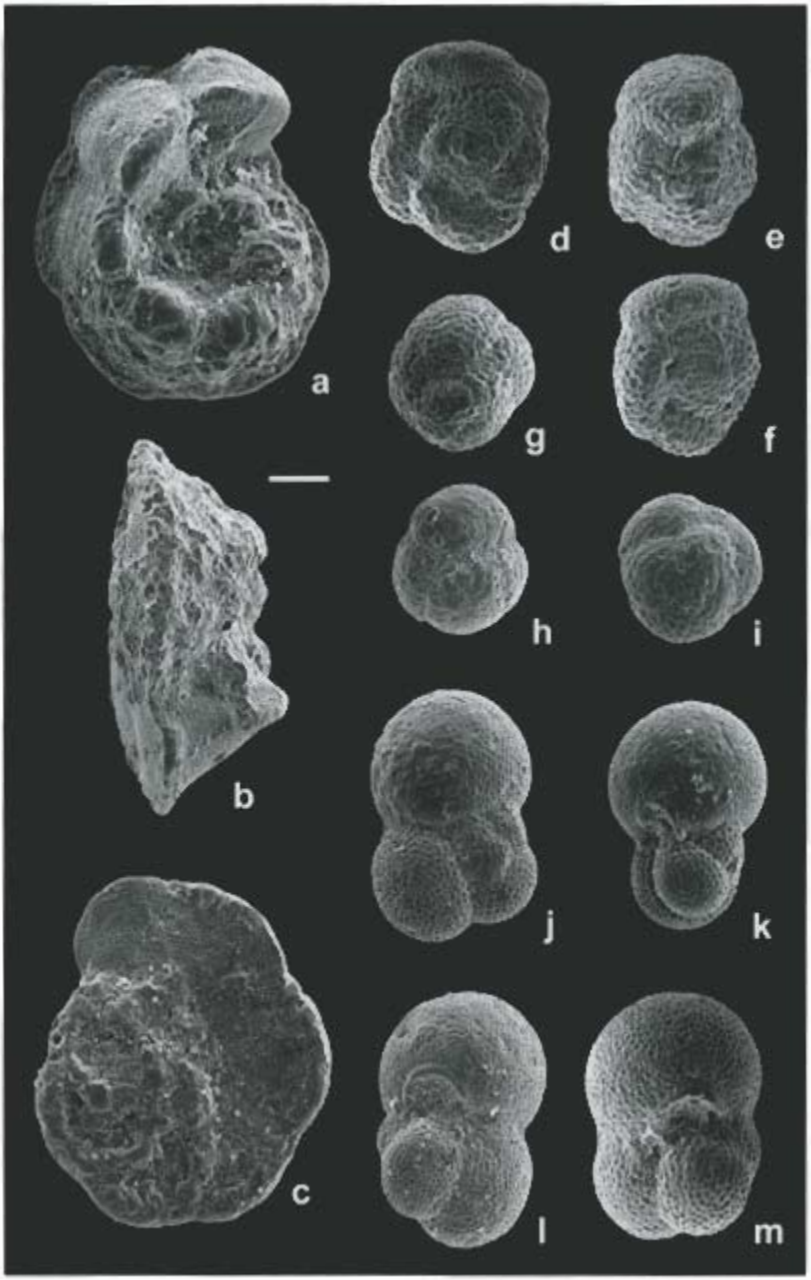

Fig. 9 (Legend see p. 86)

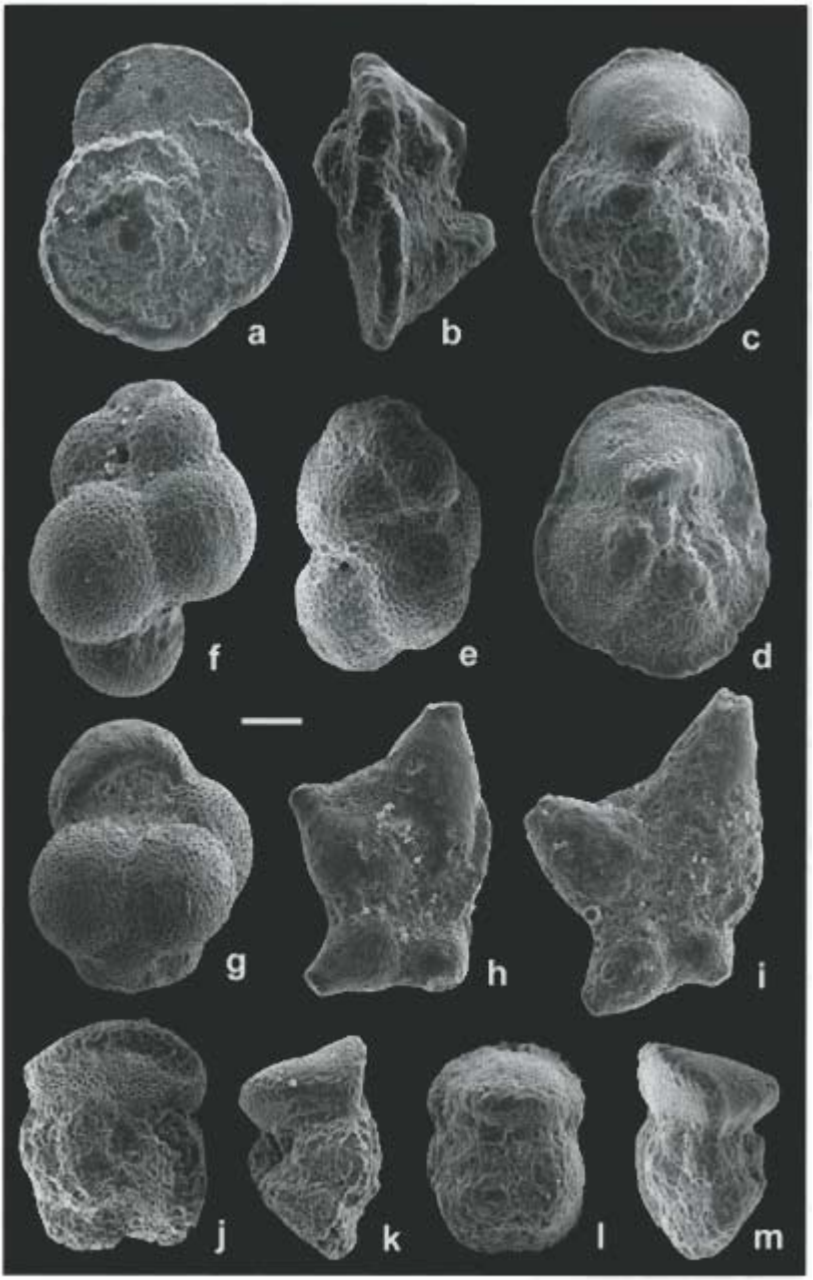

Fig. 10 (Legend see p. 89)

The simultaneous FOs of *Globigerinatheka micra* and *Morozovella gorrondatxensis* at sample Az1083 mark the base of the *Morozovella gorrondatxensis* Biozone, which extends over 125 m. The nominate taxon, originally defined in the Gorrondatxe section (ORUE-ETXEBARRIA 1985), is of great biostratigraphic interest, at least in the Pyrenean area, since its distribution is restricted to the homonymous biozone and the lower three quarters of the overlying biozone (also see CANUDO 1990; CANUDO & MOLINA 1992). The LO of *Pseudohastigerina wilcoxensis* and *Gl. indiscriminata* are recorded at the upper part of this biozone. Relatively large-sized specimens of *G. nuttalli*, showing secondary sutural apertures, appear in the uppermost part of this biozone (sample Az1185). All these characteristics suggest that the *Morozovella gorrondatxensis* Biozone mainly correlates with the upper part of Zone E7 of BERGGREN & PEARSON (2005) (equivalent to Zone P9 of BERGGREN et al. 1995), although its uppermost part corresponds to Zone E8 (= P10). The FO of *Gth. micra* in the upper part of Zone P9 was also reported by PREMOLI SILVA et al. (2003) (Fig. 1).

The FO of *Acarinina praetopilensis* in sample Az1208.5 marks the base of the homonymous biozone, which extends over 225 m. It should be noted, however, that the first specimens of the nominate taxon differ from the holotype (BLOW 1979) in that they are slightly smaller and have a less distinct circum-cameral muricocarina. The very close FOs of *A. praetopilensis* and *G. nuttalli* supports the assumption of ORUE-ETXEBARRIA & APELLANIZ (1985) that the FO of the former is a suitable event to place the Ypresian/Lutetian boundary in terms of planktonic foraminifera. The FO of a distinct morphotype of *T. frontosa*, characterized by a comparatively tight last chamber and a distinct dorsal flattening, is recorded at sample Az1292. The LO of *M. caucasica* is recorded in the middle part of this biozone, whereas those of *Subbotina inaequispira* and *M. gorrondatxensis* were found in the upper part. The *Acarinina praetopilensis* Biozone correlates with the lower part of Zone E8 of BERGGREN & PEARSON (2005).

Finally, the base of the *Hantkenina nuttalli* Biozone is defined by the FO of the nominate taxon at sample Az1433.5. It should be noted, however, that

Fig. 10. a-d) *Morozovella gorrondatxensis* (ORUE-ETXEBARRIA, 1985), a – spiral view, b – lateral view, c, d – umbilical view; **e-g)** *Guembelitrioides nuttalli* (HAMILTON, 1953), e, f – lateral view, g – umbilical view; **h-i)** *Hantkenina nuttalli* TOUMARKINE, 1981, side view; **j-m)** *Acarinina praetopilensis* (BLOW 1979), j – spiral view, k, m – lateral view, l – umbilical view. Scale bar = 100 μm.

H. nuttalli is rare in all samples. Given its rarity and the fact that its FO is located higher up than the LO of *M. caucasica*, the FO of *H. nuttalli* in the Gorrondatxe section might not correspond to its first appearance in the stratigraphic record. The FO of *Truncorotaloides topilensis* is recorded in the lower part of the *Hantkenina nuttalli* Biozone. Globigerinathekids, including *Gth. mexicana*, become very abundant 80 m higher up in the succession (see ORUE-ETXEBARRIA et al. 1984; ORUE-ETXEBARRIA & APELLANIZ 1985; PAYROS et al. 2006). All things considered, the *Hantkenina nuttalli* Biozone is correlated with the upper part of Zone E8 of BERGGREN & PEARSON (2005).

8. Nummulitids

8.1. Sampling and methods

Larger foraminifera, mostly *Nummulites* and *Assilina* specimens, as well as fragments of other shallow-water organisms (e.g., red algae and corals), occur in the basal part of many thick-bedded, mixed carbonate-siliciclastic turbidites. They occur either within rounded limestone clasts or as loose, individual grains surrounded by muddy or bioclastic matrix.

All of the turbidites in the Gorrondatxe section were examined for nummulitids. Some of them, despite bearing larger foraminifers, were not sampled because they were well cemented and individual nummulitids could not be extracted. In fact, the systematic analysis of nummulitids at specific level needs the observation of external and internal features in both microspheric and megalospheric forms. Therefore, it is necessary to have diversified populations where individual specimens can be separated. Sixteen of the Gorrondatxe turbidites fulfil these requirements, from which different types of samples were collected (Fig. 11). When possible, bulk sediment samples were collected, but in some cases individual nummulitid specimens, slabs of turbidites or limestone clasts were taken. All the samples were washed in the laboratory and as many individual nummulitid specimens as possible were separated and studied following a two-step procedure. First, their external features (diameter and shape, morphology and arrangement of

Fig. 11. Nummulitid species occurrences in the Gorrondatxe section. Broken lines on the right-hand columns indicate that the corresponding Shallow Benthic Zone is probably represented in the sample, whereas continuous lines indicate verified occurrences.

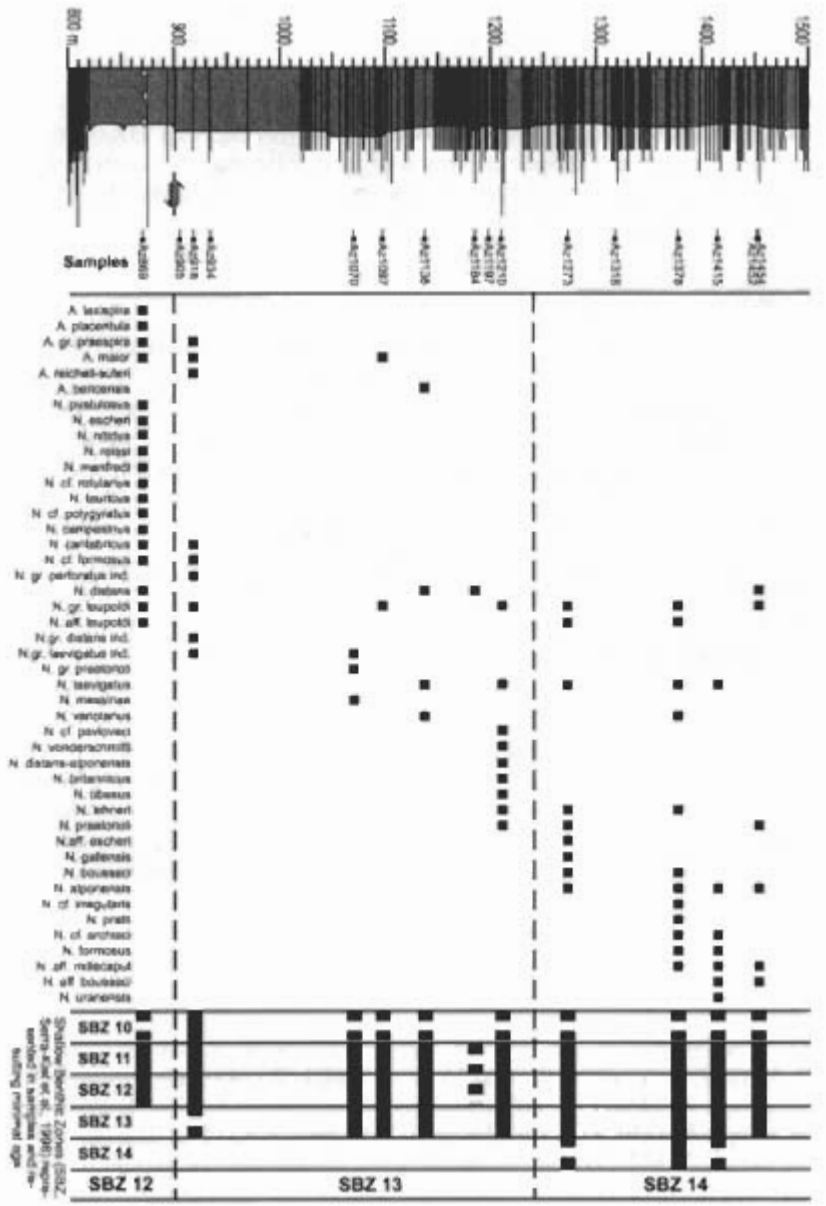

Fig. 11 (Legend see p. 90)

septal filaments and granules, etc.) were examined with a binocular microscope. Then, they were split along the equatorial section to study their internal features, such as number of whorls, rate of opening of the spire (whorl radius), number of chambers per whorl, septal and chamber shape, and the proloculus diameter of megalospheric forms (Fig. 12). Biostratigraphic range of nummulitid species was assigned following SCHAUB (1981), TOSQUELLA & SERRA-KIEL (1996) and the standard Shallow Benthic Zones (SBZ) of SERRA-KIEL et al. (1998).

8.2. Results

Four out of sixteen samples did not provide reliable results, since nummulitid specimens were poorly preserved (samples Az905, Az934, Az1197 and Az1318). The remaining twelve samples yielded a wealth of nummulitid specimens, with a total of 45 different taxa representing a mixture of resedimented and displaced faunas (Fig. 11). In fact, nummulitids from limestone clasts record the destruction and resedimentation of older, well-cemented carbonate platforms, whereas loose nummulitids are probably the result of displacement from approximately contemporaneous unconsolidated shallow-water sediments. Most of the specimens could be classified at the specific level and proved suitable for biostratigraphic determination. However, the systematic study was sometimes hindered because of the not fully diversified character of some samples. Most of the samples contained megalospheric nummulitids but lacked microspheric forms. This situation is probably the result of the hydrodynamic sorting (i.e., grain-size classification) of the sediment involved in turbidity currents, which led to the accumulation of large microspheric and small megalospheric nummulitid tests separately. Therefore, since complete nummulitid populations are not represented, a precise systematic determination was sometimes difficult to

Fig. 12. a) *Nummulites lorioli*, A-form, sample Az1378; **b)** *N. boussaci*, A-form, sample Az1273; **c)** *N.* aff. *millecaput*, A-form, sample Az1452; **d)** *N. alponensis*, A-form, sample Az1452; **e)** *N.* aff. *boussaci*, A-form, sample Az1273; **f)** *N. obesus*, B-form, sample Az1210; **g)** *N. variolarius*, A-form, sample Az1138; **h)** *N. messinae*, A-form, sample Az1070; **i)** *N. laevigatus*, A-form, sample Az1210; **j)** *N. praelorioli*, A-form, sample Az1273; **k)** *Assilina bericensis*, A-form, sample Az1138; **l)** *N. gallensis*, A-form, sample Az1273; **m)** *N. manfredi*, B-form, sample Az869; **n)** *N. manfredi*, A-form, sample 869; **o)** *A. maior*, A-form, sample Az869; **p)** *N. formosus*, A-form, sample Az1378. Scale bars = 1 mm.

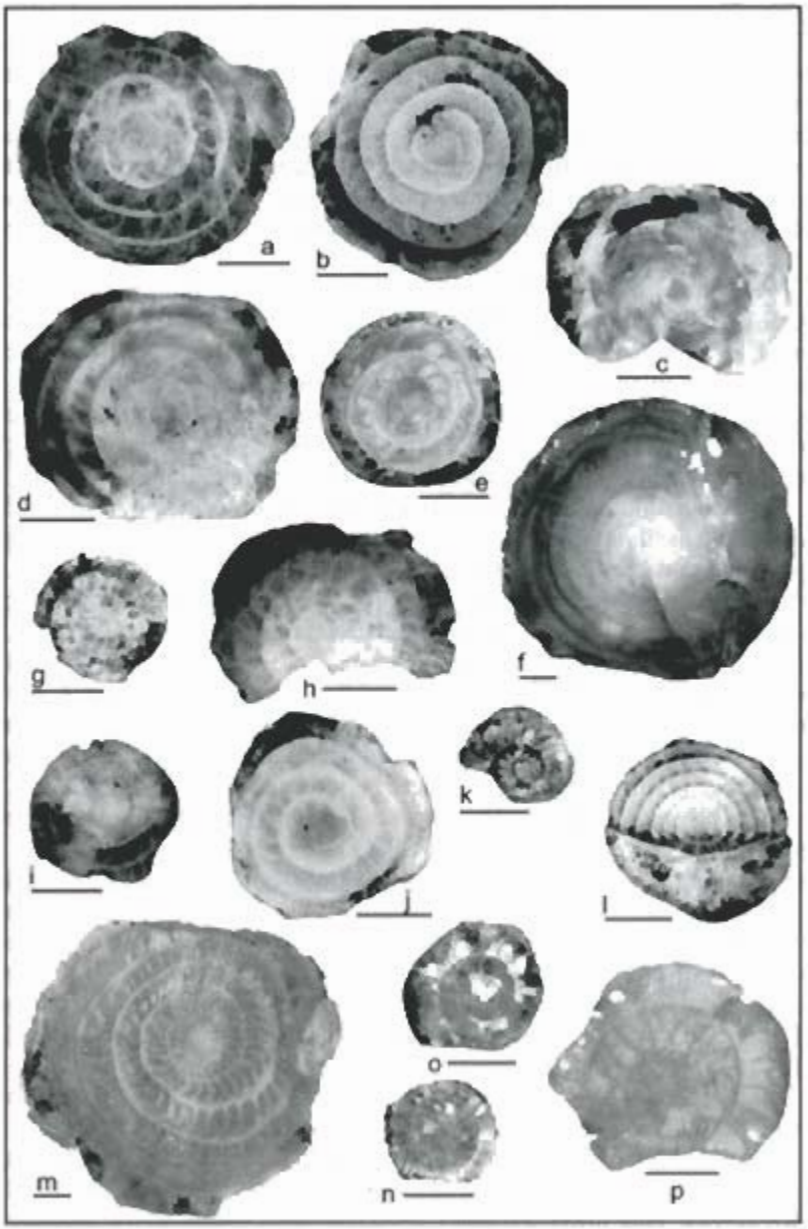

Fig. 12 (Legend see p. 92)

obtain. That is why the terms "cf." (= confer), "gr." (= group) and "aff." (= affinis) are used in some cases. On the other hand, the most evolved morphotypes of a phylogenetic series were easy to recognize. In general, the most modern specimens are larger and show more complex test ornamentation. However, it is not straightforward to apply this rule to small-sized microspheric nummulitids, since small test size and simple ornamentation might be related either to a lower phylogenetic level (i.e. stratigraphically older specimens) or, alternatively, to the younger ontogenetic stage of more modern specimens.

These facts, along with the unspecific biostratigraphic range of some species, sometimes made it difficult to distinguish whether a sample contained a homogenous association, with specimens belonging to a single biozone, or a mixed association with specimens belonging to more than one biozone. However, although these limitations hamper the precise reconstruction of the paleobiocenosis at some levels, it was still possible to date the youngest possible age of the turbidites containing nummulitids (Fig. 11).

The association observed in sample Az 869 is constituted by: *Nummulites pustulosus, Assilina placentula* and *A.* cf. *reicheli*, taxa with a biostratigraphic range that spans SBZ10 and SBZ11; *N. escheri, N.* gr. *leupoldi, N.* cf. *rotularius* and *A.* gr. *praespira*, with a range from SBZ10 to SBZ12; *N. tauricus, N. nitidus* and *A. laxispira*, characterizing SBZ11; *N. distans, N. reissi, N.* cf. *polygyratus*, ranging between SBZ11 and SBZ12; and *N. campsesimus, N. manfredi, N.* aff. *leupoldi, N.* cf. *formosus*, and *A. maior*, characteristic of SBZ12. Therefore, sample Az 869 presents an association of nummulitids that characterizes SBZ11 and SBZ12, as well as some species of unspecific biostratigraphic range between SBZ10 and SBZ11 that, possibly, belong to SBZ11. This association indicates SBZ12 as minimum age, with faunas resedimented from SBZ11.

Sample Az 918 presents a nummulitid association constituted by *Nummulites cantabricus* (SBZ11), *N.* gr. *leupoldi* (SBZ10-12), *Assilina reicheli-suteri* (SBZ12-13), *N.* cf. *formosus* and *A. maior* (SBZ12). In addition, specimens of the *N. perforatus, N. laevigatus, N. distans* and *A. praespira* groups were observed, which show characteristics attributable to zones SBZ12-13. Therefore, it was not possible to accurately place the boundary between these two zones.

Samples Az1070, Az1097, Az1138, Az1184 and Az1210 yielded a nummulitid association constituted by *N. vonderschmitti, N. gr. leupoldi* and *N.* cf. *pavloveci* (SBZ10-12), *N. distans* (SBZ11-12), *A. maior* (SBZ12), *N. praelorioli* and *N. distans-alponensis* (SBZ11-13), *N.* gr. *laevigatus* indet. (SBZ12-13), and lower Lutetian (SBZ13) taxa, such as *N. obesus, N. lehneri, N. messinae, N. laevigatus, N. britannicus, N. variolarius* and *A. bericensis*.

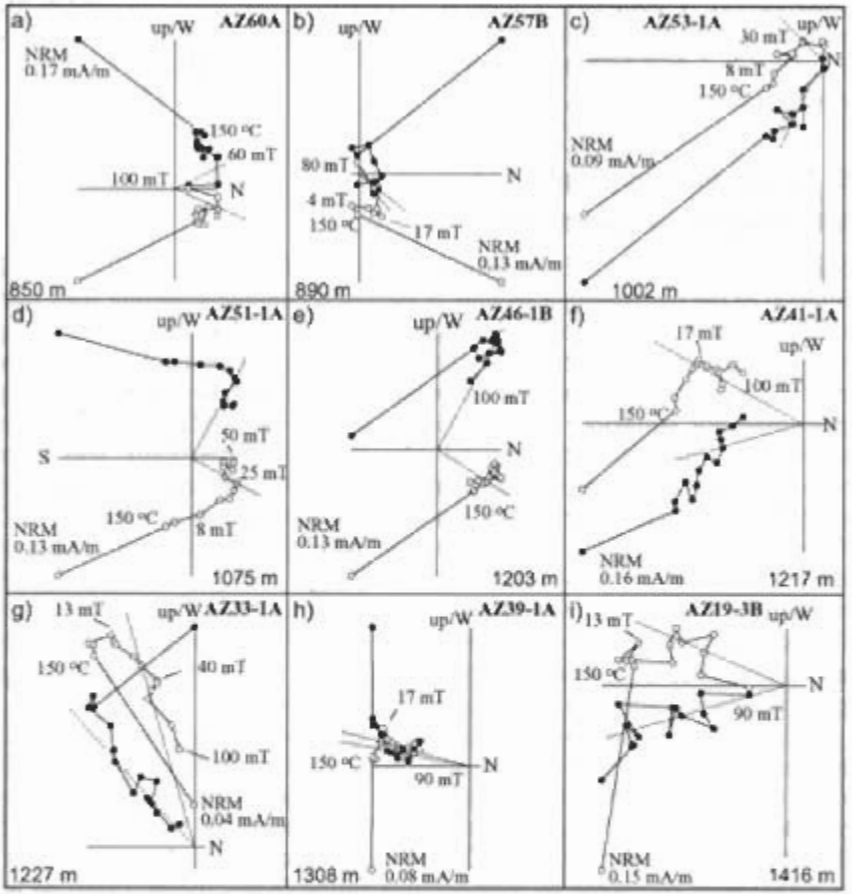

Fig. 13. Bedding-corrected orthogonal plots of demagnetization data from representative specimens from the Gorrondatxe section. Solid (open) symbols represent projections onto the horizontal (vertical) plane. The stratigraphic level, the fitted ChRM direction, the NRM intensity and some demagnetization treatments are indicated.

Finally, samples Az1273, Az1378, Az1415, Az1452 and Az1454 contain a nummulitid association constituted by *N.* gr. *leupoldi*, *N.* cf. *archiaci* and *N.* cf. *irregularis* (SBZ10-12); *N. distans* and *N. pratti* (SBZ11-12); *N. formosus*, *N.* aff. *leupoldi* and *N.* aff. *escheri* (SBZ12); *N. praelorioli*

(SBZ12-13); *N. gallensis, N. lehneri, N. laevigatus, N. alponensis* and *N.* aff. *millecaput* (SBZ13); *N. uranensis* (SBZ13 and base of SBZ14); and a *N. boussaci-lorioli* morphotype characteristic of biozone SBZ14 (lowermost middle Lutetian).

9. Magnetostratigraphy

9.1. Sampling and methods

Sampling for magnetostratigraphy was conducted throughout a 700 m thick interval of the Gorrondatxe section. A total of 65 unique sampling sites were obtained, comprising 2 to 3 hand-samples per site. Paleomagnetic sampling was basically restricted to the hemipelagic lithologies (mostly grey marls and marly limestones), which are potentially more suitable facies regarding paleomagnetic behaviour in comparison with turbidites. Hand-samples were oriented *in situ* with a compass and subsequently standard cubic specimens were cut in the laboratory for analysis. Natural remanent magnetization (NRM) and remanence through demagnetization were measured on a 2G Enterprises DC SQUID high-resolution passthrough cryogenic magnetometer (manufacturer noise level of 10^{-12} Am^2) operated in a shielded room at the Istituto Nazionale di Geofisica e Vulcanologia (INGV) in Rome, Italy. A Pyrox oven in the shielded room was used for thermal demagnetizations and alternating field (AF) demagnetization was performed with three orthogonal coils installed inline with the cryogenic magnetometer.

Paleomagnetic analysis was conducted on 116 specimens corresponding to 1 or 2 specimens per sampling site. Progressive stepwise alternating field (AF) demagnetization was routinely used and applied after a single heating step to 150°C. AF demagnetization included 14 steps (4, 8, 13, 17, 21, 25, 30, 35, 40, 45, 50, 60, 80, 100 mT). Characteristic remanent magnetizations (ChRM) were computed by least-squares fitting (Kirschvink 1980) on the orthogonal demagnetization plots (Zijderveld 1967). The ChRM declination and inclination for each sample has been used to derive the latitude of the virtual geomagnetic pole (VGP). This parameter has been used as an indicator of the polarity (normal polarity for positive VGP latitudes and reverse polarity for negative VGP latitudes).

9.2. Results

The NRM intensities are on the order of 0.1 mA/m, usually decreasing to 50 % or less at 150°C (Fig. 13). The characteristic remanent magnetization (ChRM) is conventionally defined as the linear segment trending towards the origin of the demagnetization diagram. Normally (class A samples), the

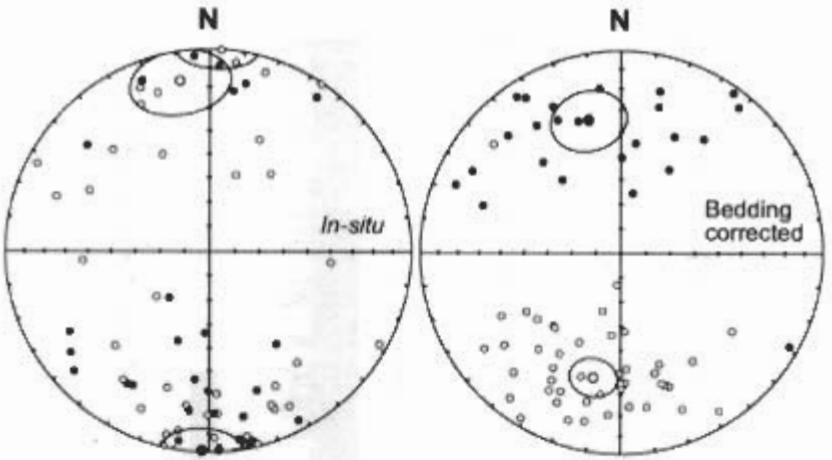

Sample	N	Dec.	Inc.	k	α_{95}
Group N	23	350.1	-15.6	4.4	16.3
Group R	46	182.0	0.9	4.3	11.5
All	69	358.1	-5.9	4.2	9.5

Sample	N	Dec.	Inc.	k	α_{95}
Normal	23	346.1	32.8	5.9	13.7
Reverse	46	192.3	-36.4	6.8	8.7
All	69	3.5	35.8	6.0	7.6

Fig. 14. Equal-area projections of the ChRM directions before (*in-situ*) and after bedding correction. The 95 % confidence ellipse for the normal and reverse mean directions is indicated. Statistical information is given (N, number of samples; Dec., declination; Inc., inclination; k, Fisher's precision parameter; α_{95}, radius of the 95 % confidence cone).

ChRM component can be isolated above 13-17 mT after removal of a viscous secondary component at low fields that conforms to the recent Earth's magnetic field in geographic (in-situ) coordinates. The ChRM component most likely resides in a low-coercivity mineral like maghemite or magnetite although a minor contribution of a higher coercivity mineral (iron-sulphide, hematite?) cannot be ruled out considering that in some instances (Fig. 13e and g) the ChRM is not fully demagnetized at the highest applied magnetic field (100 mT). The ChRM components present either normal (Fig. 13a-b, d-e) or reverse (Fig. 13c, f-i) polarity in bedding-corrected coordinates (Fig. 14). In a few cases, the calculated ChRM has been regarded as unreliable (class B samples) (Fig. 15). We consider the demagnetization

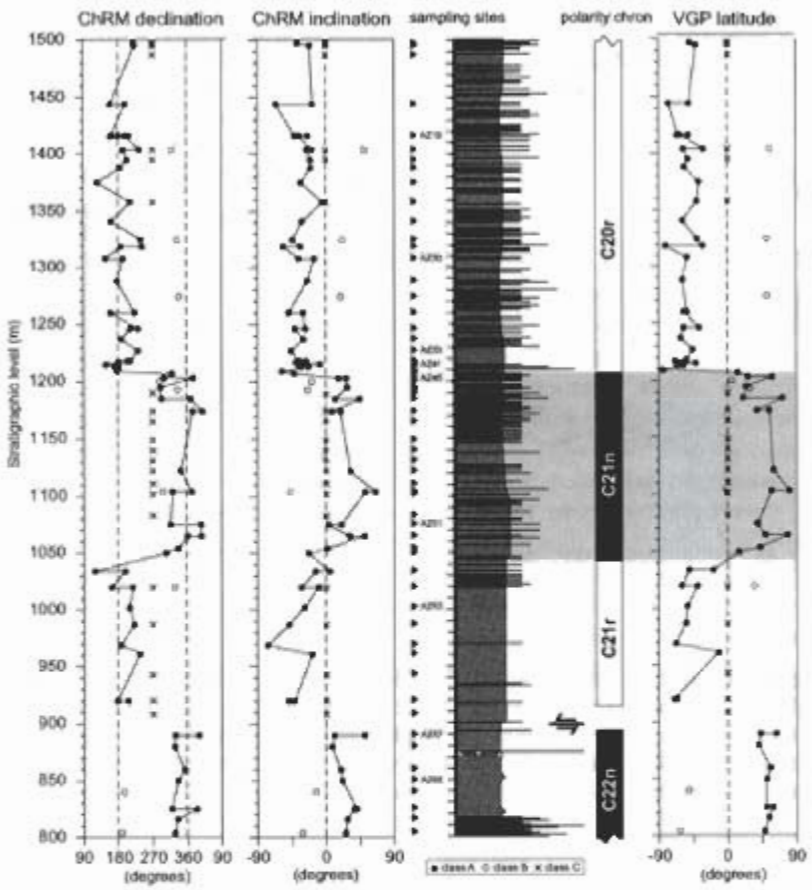

Fig. 15. Stratigraphic variation of the ChRM directions and virtual geomagnetic pole (VGP) latitude and interpreted magnetic polarity stratigraphy plotted on a lithologic log of the Gorrondatxe section.

behavior as unsuitable for magnetostratigraphic interpretation in 30 % of the analyzed specimens (class C samples) which mostly relate to very weak samples (Fig. 15). The magnetostratigraphy is based on Class A samples (Fig. 15).

The reversal test of McFADDEN & McELHINNY (1990) has been performed on the ChRM components in order to assess the antipodality of the normal and reverse populations (Fig. 15). This test classifies a 'positive' reversal test on the basis of the angle γ_c between the mean directions of the two sets of observations at which the null hypothesis of a common mean direction would be rejected with 95 % confidence (class 'A' if $\gamma_c \leq 5°$ as 'B' if $5° < \gamma_c \leq 10°$, as 'C' if $10° \leq \gamma_c \leq 20°$, and 'Indeterminate' if $\gamma_c > 20°$). The ChRM data for the Gorrondatxe section passes the reversal test as class C ($\gamma_c = 16.2°$).

The primary nature of the ChRM is supported by: 1) the presence of a dual-polarity ChRM in addition to the low temperature present-day field overprint; 2) an unrealistic shallow inclination before bedding correction (Fig. 14) (e.g. not compatible with any geomagnetic Cenozoic field direction for Iberia); 3) changes in polarity do not seem to be lithologically controlled.

The VGP latitude derived from the ChRM directions yields a succession of four magnetozones (two normal and two reverse). The lower normal magnetozone, which correlates with planktonic foraminifer zones P9 and E7, calcareous nannofossil zones CP11-CP12a, and larger foraminifer zone SBZ12 can be directly correlated to chron C22n. The overlying reverse magnetozone is correlated to chron C21r based on its stratigraphic position above the interval interpreted as chron C22n and on the basis of calcareous nannofossil and nummulitid biostratigraphic data. The succeeding normal and reverse magnetozones correspond to chrons C21n and C20r, respectively, on the same basis.

10. Discussion

10.1. Positioning the Ypresian/Lutetian boundary

All the events traditionally used to place the Ypresian/Lutetian boundary (i.e., the planktonic foraminifer P9 (= E7) / P10 (= E8) Zone boundary; the calcareous nannofossil CP12a / CP12b Subzone boundary; the larger foraminifer SBZ12 / SBZ13 Zone boundary; and the boundary between magnetic polarity chrons C22n and C21r) have been identified in the Gorrondatxe section (Fig. 16). However, a comparison of the Gorrondatxe data with the standard biomagnetostratigraphic scheme shown in Fig. 1 evidences that all these events, previously considered as simultaneous, actually occur at very different levels. A concomitant consequence arising from that observation is that before selecting a section to place the Ypresian/Lutetian boundary stratotype, the criterion to identify this boundary should be precisely defined. A first step should be the description of the succession of the events that characterizes the Ypresian/Lutetian boundary interval,

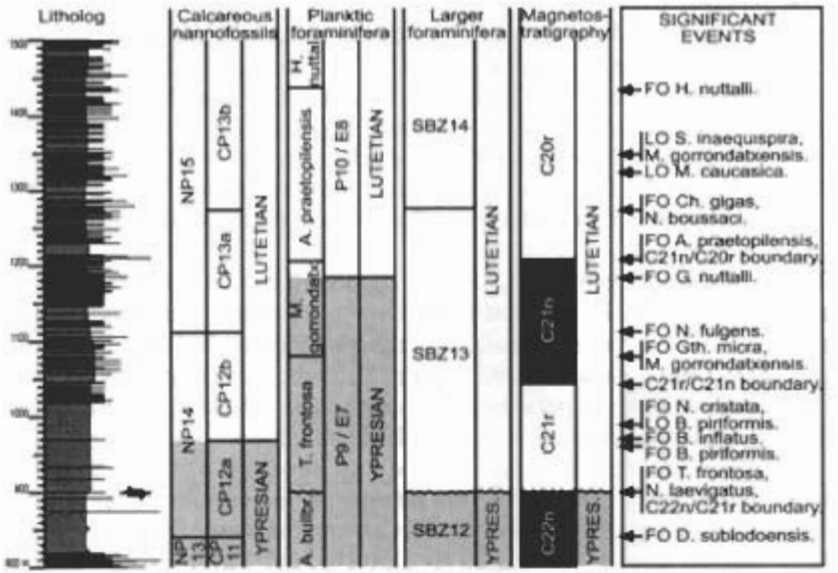

Fig. 16. Summary of the biostratigraphy (calcareous nannofossils, planktonic foraminifera and larger foraminifera) and magnetostratigraphy in the Gorrondatxe section. The position of the boundary between the Ypresian (grey) and Lutetian (white) stages varies depending on the scale. The most important events traditionally used or suitable for defining the Ypresian/Lutetian boundary are depicted in the right-hand box.

which in this work has been informally considered as extending from the FO of *D. sublodoensis* to the FO of hantkeninids. Evaluating the pros and cons, and evaluating the usefulness of each of these events is beyond the scope of this paper, as this decision is the domain of the International Subcommission on Paleogene Stratigraphy (ISPS). Therefore, only the relative position of the different events suitable to be selected as "official" markers of the Y/L boundary, and their correlation with other zonal scales, will be highlighted below.

The tops of magnetic polarity chron C22n and larger foraminifer Zone SBZ12, previously used to define the Y/L boundary by magnetostratigra-

phers and paleontologists working with larger foraminifera respectively, are not preserved in the Gorrondatxe section due to a fault at 900 m of the succession (Fig. 16). However, these events are found to occur within calcareous nannofossil Zone CP12a, as already shown in the standard correlation scheme (Fig. 1), within planktonic foraminifera Zone E7 (= P9), and seem to be approximately coeval with the FO of the planktonic foraminifer *T. frontosa*.

The FO of *B. inflatus* is the most suitable calcareous nannofossil marker event to characterize the Y/L boundary, having the additional advantage of preserving the current concept of the Lutetian stage. In fact, calcareous nannofossil studies carried out in the original Lutetian stratotype in Paris provided an assemblage indicative of Zone CP12b (AUBRY 1986), whose base is marked by the FO of *B. inflatus*. In the Gorrondatxe section that event is well constrained at 969 m, and occurs within the upper part of chron C21r, the planktonic foraminiferal *T. frontosa* Biozone (upper part of E7), and within larger foraminiferal zone SBZ13 (Fig. 16). Several additional calcareous nannofossil events have been identified slightly lower and higher in the succession (Figs. 4, 16). Relatively close to the FO of *B. inflatus* we found the FO of *T. frontosa*, poorly documented in the Gorrondatxe section due to the fault at 900 m, and the FOs of *Gth. micra* and *M. gorrondatxensis* at 1083 m.

Based on planktonic foraminifera, the Ypresian/Lutetian boundary is marked by the supposedly simultaneous FOs of specimens belonging to the genus *Hantkenina* and *G. nuttalli* (BERGGREN & PEARSON 2005) (Fig. 1). However, these events are very distant from each other in the Gorrondatxe section (Figs. 8, 16). The FO of *G. nuttalli* is recorded at 1185 m, relatively close to the FO of *A. praetopilensis* at 1208.5 m. These two events occur at the uppermost part and at the upper boundary of chron C21n, respectively; in the middle part of calcareous nannofossil Zone CP13a, which extends from 1107 to 1269 m; and within the upper part of larger foraminifer Zone SBZ13. The FO of hantkeninids is recorded at 1433.5 m, being correlatable with chron C20r, calcareous nannofossil Zone CP13b, and larger foraminiferal Zone SBZ14. However, in accordance with the opinions of ORUE-ETXEBARRIA & APELLANIZ (1985), PREMOLI SILVA & BOERSMA (1988), COXALL et al. (2003) and BERGGREN & PEARSON (2005), the FO of hantkeninids in the Gorrondatxe section might probably be younger than their effective first appearance in the stratigraphic record. It should be noted, however, that the FO of hantkeninids well after the FO of *G. nuttalli* has also been reported in other areas (e.g., PREMOLI-SILVA et al. 2003).

10.2. Suitability of the Gorrondatxe section for the GSSP of the base of the Lutetian

The Gorrondatxe section satisfies most of the infrastructural, biostratigraphic and geological requirements listed by the International Commission on Stratigraphy (ICS) (REMANE et al. 1996), as demonstrated above. In particular, the great sedimentary thickness is one of the most outstanding features in favour of selecting the Gorrondatxe section as the GSSP of the base of the Lutetian. Table 1 shows the thicknesses of selected biostratigraphic and magnetostratigraphic zones in the Ypresian/Lutetian boundary interval of the Gorrondatxe section and in other well-documented successions, some of which have already been proposed as candidates for the GSSP of the base of the Lutetian. Table 1 readily demonstrates that the Gorrondatxe section is much thicker than all the other sections, a feature that indicates a much higher sedimentation rate. Hence, successive biostratigraphic and magnetostratigraphic events are better individualized in the Gorrondatxe section and their chronological succession can be more easily established than in all other sections that have been described until now (Fig. 16). Such a great thickness is the result of abundant intercalations of turbiditic beds (Figs. 3, 16). However, these turbidites do not diminish the suitability of the Gorrondatxe section as a candidate for the GSSP of the base of the Lutetian, since they are generally extensive, tabular-shaped and flat-based, recording therefore the effect of turbidity currents with low erosive capacity, which did not cause any significant disturbance on the sea floor. Quite to the opposite, some of these turbidity currents supplied abundant nummulitids, allowing thus the improvement of the correlation between larger foraminiferal and calcareous planktonic biostratigraphic zonations. Since larger foraminifera are transitional between open marine and terrestrial faunas, they could eventually prove invaluable for the correlation of biostratigraphic zonal schemes based on open marine planktonic organisms with those from continental areas.

The only problem with the Gorrondatxe section is the fault located at 900 m. In fact, the tops of chron C22n and larger foraminiferal zone SBZ12 are not preserved in the Gorrondatxe section due to that fault (Fig. 16). Therefore, in the case of selection of either of these two events as marker event for the Ypresian/Lutetian boundary, the Gorrondatxe section would not be an appropriate candidate for the corresponding GSSP. It should be noted, however, that these two events are now known to be older than the base of the original Lutetian stratotype in Paris.

If the base of Zone CP12b (marked by the FO of *B. inflatus*) were chosen as the Ypresian/Lutetian boundary marker event, the Gorrondatxe section should be considered as a firm candidate for the GSSP, since that event has

Table 1. Stratigraphic characteristics of selected sections displaying the Ypresian/Lutetian boundary interval. Duration of magnetic and biostratigraphic zones from LUTERBACHER et al. (2004).

SECTION	C21n (1.389 m.y.)	CP12a (1.0 m.y.)	CP12b (1.2 m.y.)	CP13a (1.6 m.y.)	P10 / E8 (3.7 m.y.)
Gorrondatxe	Thickness: 166 m; sedimentation rate: 87.88 m/m.y.	Thickness > 129 m; sedimentation rate > 129 m/m.y.	Thickness: 142 m; sedimentation rate: 118.33 m/m.y.	Thickness: 162 m; sedimentation rate: 101.25 m/m.y.	Thickness: 538 m; sedimentation rate: 145.41 m/m.y.
Chaumont-en-Vexin, Oise, Paris Basin (AUBRY 1986)	Not specified	Not preserved	Thickness: 9.5 m (base is probably missing); sedimentation rate: 7.3 m/m.y.	Not specified	Not specified
Whitecliff Bay, Hampshire-London Basin	Thickness: 18.5 m; sedimentation rate: 9.79 m/m.y. (TOWNSEND & HAILWOOD 1985; AUBRY et al. 1986)	Not preserved	Identified, but thickness not specified (AUBRY 1986)	Not specified	Not specified
Contessa Highway, Italy (LOWRIE et al. 1982)	Thickness: 13 m; sedimentation rate: 6.88 m/m.y.	Not specified	Not specified	Not specified	Thickness: 26 m; sedimentation rate: 7.03 m/m.y.
Contessa Road, Italy (LOWRIE et al. 1982)	Thickness: 11.3 m; sedimentation rate: 5.98 m/m.y.	Not specified	Not specified	Not specified	Not specified
Bottaccione, Italy	Thickness: 8.25 m (NAPOLEONE et al. 1983); sedimentation rate: 4.37 m/m.y.	Thickness: 25.5 m (MONECHI & THUNELL 1985); sedimentation rate: 25.5 m/m.y.	Thickness: 2 m, but FO of *A. inflatus* does probably not coincide with FAD (MONECHI & THUNELL 1985); sedimentation rate: 1.54 m/m.y.	Not specified	Thickness: 24 m (NAPOLEONE et al. 1983); sedimentation rate: 6.49 m/m.y.
Agost, Spain (MOLINA et al. 2000)	Not specified	Thickness: 16.9 m; sedimentation rate: 16.9 m/m.y	Thickness: 15.83 m; sedimentation rate: 12.18 m/m.y.	Not precisely defined; maximum possible thickness: 11 m; sedimentation rate: 6.67 m/m.y.	Thickness 23.75 m; sedimentation rate: 6.42 m/m.y. Composite thickness of *A. praeplanisensis* and P10 *zona alveata* zones: 47.5 m; sedimentation rate: 12.84 m/m.y.
Fortuna, Spain (GONZALVO et al. 2001)	Not specified	Not specified	Not specified	Not specified	Thickness of *H. nuttalli* Zone: 21.42 m; sedimentation rate: 5.79 m/m.y. Composite thickness of *A. praeplanisensis* and *H. nuttalli* zones: 28.05 m; sedimentation rate: 7.58 m/m.y.
Possagno, Italy (AGNINI et al. 2006)	Thickness: 18 m; sedimentation rate: 9.63 m/m.y.	Thickness: 22.8-27.4 m; sedimentation rate: 10.36-12.45 m/m.y.		Thickness: 6.9 m; sedimentation rate: 4.18 m/m.y.	Not specified

been accurately located and correlated with other scales (Fig. 16). Based on the same line of reasoning, the same conclusion would be also valid, if the base of planktonic foraminiferal Zone E8 (marked by the FO of *G. nuttalli*, and supposedly correlatable with Zone P10 as marked by the FO of hantkeninids) would be the selected marker event.

11. Summary and Conclusions

A high-resolution multi-disciplinary study, including physical stratigraphy (lithostratigraphy, sequence stratigraphy and magnetostratigraphy) and biostratigraphy (calcareous nannofossil, planktonic foraminifer and larger foraminifera), has been carried out in the 700 m thick uppermost Ypresian – lower Lutetian interval of the Gorrondatxe section. The results show that the different events traditionally used to place the Ypresian/Lutetian boundary, hitherto thought to be virtually simultaneous (i.e., the planktonic foraminiferal P9 (= E7) / P10 (= E8) zonal boundary; the calcareous nannofossil CP12a / CP12b subzonal boundary; the larger foraminiferal SBZ12 / SBZ13 zonal boundary; and the boundary between magnetic polarity chrons C22n and C21r), actually occur at very different levels. Therefore, before considering any section to place the Ypresian/Lutetian boundary stratotype, the International Subcommission on Paleogene Stratigraphy should decide on the criterion to precisely define this boundary. To this end, the succession of events pinpointed in the Ypresian/Lutetian boundary interval of the Gorrondatxe beach section might prove to be a useful database (Fig. 16).

The Gorrondatxe section fulfils most of the infrastructure, biostratigraphic and geological requirements required of a prospective stratotype section by the International Commission on Stratigraphy. In addition, the great sedimentary thickness, which implies a deep-marine sedimentation rate about ten times higher than in other Ypresian/Lutetian boundary sections (Table 1), provides the Gorrondatxe section an additional value, as it offers the opportunity to chronologically order successive biomagnetostratigraphic events more precisely than elsewhere. The only drawback with the Gorrondatxe section is that the "true" tops of chron C22n and larger foraminiferal Zone SBZ12 are not preserved due to a fault. Otherwise, all other possible Ypresian/Lutetian boundary marker events have been precisely pinpointed in the Gorrondatxe section. Therefore, we consider that, once the criterion to define the Ypresian/Lutetian boundary is selected, the Gorrondatxe beach section should be considered as a firm candidate to place the Global Stratotype Section and Point of the base of the Lutetian Stage.

Acknowledgements

The authors thank the referee HANSPETER LUTERBACHER for his helpful suggestions to improve the manuscript and EUSTOQUIO MOLINA for his very positive comments. Field and laboratory works were funded by Research Projects CGL2005-02770/ BTE, CGL2005-01721/ BTE (Ministry of Science and Technology, Spanish Government) and 9/UPV00121.310-1455/2002 (University of the Basque Country). G.B. acknowledges support through a Basque Government postdoctoral grant.

References

AGNINI, C., MUTTONI, G., KENT, D. V. & RIO, D. (2006): Eocene biostratigraphy and magnetic stratigraphy from Possagno, Italy: the calcareous nannofossil response to climate variability. – Earth Planet. Sci. Lett., **241**: 815-830.

AUBRY, M.-P. (1983): Biostratigraphie du Paléogène épicontinental de l'Europe du Nord-Ouest: Étude Fondée sur les Nannofossiles Calcaires. – Doc. Lab. Géol. Lyon, **89**: 1-317.

– (1986): Paleogene calcareous nannoplankton biostratigraphy of Northwestern Europe. – Palaeogeogr., Palaeoclimatol., Palaeoecol., **55**: 267-334.

– (1995): From chronology to stratigraphy: interpreting the Lower and Middle Eocene stratigraphic record in the Atlantic ocean. – In: BERGGREN, W. A., KENT, D. V., AUBRY, M.-P. & HARDENBOL, J. (Eds.): Geochronology, Time Scales and Global Stratigraphic Correlation. – SEPM Spec. Publ., **54**: 213-274.

AUBRY, M.-P., HAILWOOD, E. A. & TOWNSEND, H. A. (1986): Magnetic and calcareous-nannofossil stratigraphy of the lower Palaeogene formations of the Hampshire and London basins. – J. Geol. Soc. London, **143**: 729-735.

BERGGREN, W. A. (1972): A Cenozoic time-scale: some implications for regional geology and paleobiogeography. – Lethaia, **5**: 195-215.

BERGGREN, W. A. & MILLER, K. G. (1988): Paleogene tropical planktonic foraminiferal biostratigraphy and magnetobiochronology. – Micropaleontology, **34**: 362-380.

BERGGREN, W. A. & PEARSON, P. N. (2005): A revised tropical to subtropical Paleogene planktonic foraminiferal zonation. – J. Foram. Res., **35**: 279-298.

BERGGREN, W. A., KENT, D. V., SWISHER, C. C. & AUBRY, M.-P. (1995): A revised Cenozoic geochronology and chronostratigraphy. – In: BERGGREN, W. A., KENT, D. V., AUBRY, M.-P. & HARDENBOL, J. (Eds.): Geocheonology, Time Scales and Global Stratigraphic Correlation. – SEPM Spec. Publ., **54**: 129-212.

BLONDEAU, A., CAVELIER, C., LABOURGUIGNE, J., MEGNIEN, C. & MEGNIEN, F. (1980): Eocène moyern. – In: MEGNIEN, C. & MEGNIEN, F. (Eds.): Synthèse géologique du Bassin de Paris. – Mém. Bur. Rech. Géol. Min., **103**: 367-377.

BLOW, W. H. (1979): The Cenozoic Globigerinida: a study of the morphology, taxonomy, evolutionary relationships and the stratigraphical distribution of some Globigerinida (mainly Globigerinacea). – 1413 pp.; Leiden (Brill).

BOWN, P. R. (1998): Calcareous Nannofossil Biostratigraphy. – 315 pp., British Micropalaeontological Society Publication Series; London (Chapman and Hall & Kluwer Academic Publisher).

Bown, P. R. (2005): Palaeogene calcareous nannofossils from the Kilwa and Lindi areas of coastal Tanzania (Tanzania Drilling Project 2003-4). – J. Nannoplankton Res., **27** (1): 21-95.

Bramlette, M. N. & Sullivan, F. R. (1961): Coccolithophorids and related nannoplankton of the early Tertiary in California. – Micropaleontology, **7**:129-174.

Canudo, J. I. (1990): Los foraminíferos planctónicos del Paleoceno-Eoceno en el Prepirineo meridional y su comparación con la cordillera Bética (Ph.D. thesis, Univ. Zaragoza). – 436 pp; Zaragoza.

Canudo, J. I. & Molina, E. (1992): Bioestratigrafiia con foraminíferos planctónicos del Paleógeno del Pirineo. – N. Jb. Geol. Paläont., Abh., **186**: 97-135.

Coxall, H. K., Huber, B. T. & Pearson, P. N. (2003): Origin and morphology of the Eocene planktonic foraminifer *Hantkenina*. – J. Foram. Res., **33**: 237-261.

De Lapparent, A. (1883): Traité de géologie. – 1280 pp.; Paris (Savy).

Erbacher, J., Mosher, D. C., Malone, M. J., Berti, D., Bice, K. L., Bostock, H., Brumsack, H. J., Danelian, T., Forster, A., Glatz, C., Heindersdorf, F., Henderiks, J., Janecek, T. R., Junium, C., Le Callonec, L., MacLeod, K., Meyers, P. A., Mutterlose, H. J., Nishi, H., Norris, R. D., Ogg, J. G., O'Regan, A. M., Rea, B., Sexton, P., Sturt, H., Suganuma, Y., Thurow, J. W., Wilson, P. A. & Wise, S. W. Jr. (2004): Demara Rise: Equatorial Cretaceous and Paleogene paleoceanographic transect, western Atlantic. – Proc. ODP, Init. Rep., **207** [http://www-odp.tamu.edu/publications/207-IR/207ir.htm].

Gonzalvo, C., Mancheño, M. A., Molina, E., Rodríguez-Estrella, T. & Romero, G. (2001): El límite Ypresiense/Luteciense en la Región de Murcia (Cordillera Bética, España). – Geogaceta, **29**: 65-68.

Hardenbol, J. & Berggren, W. A. (1978): A new Paleogene numerical time scale. – In: Cohee, G. V., Glaessner, M. F. & Hedberg, H. D. (Eds.): Contributions to the geologic time scale. – Amer. Assoc. Petrol. Geol., Stud. Geol., **6**: 213-234.

Kirschvink, J. L. (1980): The least-square line and plane and analysis of paleomagnetic data. – Geophys. J. Astron. Soc., **62**: 699-718.

Lowrie, W., Alvarez, W., Napoleone, G., Perch-Nielsen, K., Premoli Silva, I. & Toumarkine, M. (1982): Paleogene magnetic stratigraphy in Umbrian pelagic carbonate rocks: the Contessa sections, Gubbio. – Geol. Soc. Amer. Bull., **93**: 414-432.

Luterbacher, H. P., Ali, J. R., Brinkuis, H., Gradstein, F. M., Hooker, J. J., Monechi, S., Ogg, J. G., Powell, J., Röhl, U, Sanfilippo, A. & Schmitz, B. (2004): The Paleogene Period. – In: Gradstein, F. M., Ogg, J. G. & Smith, A. G. (Eds.): A geologic time scale 2004, p. 384-408; Cambridge (Cambridge Univ. Press).

Lyle, M. W., Wilson, P. A., Janacek, T. R., Backman, J., Busch, W. H., Coxall, H. K., Faul, K., Gaillot, P., Hovan, S. A., Knoop, P., Kruse, S., Lanci, L., Lear, C., Moore, T. C., Nigrini, C. A., Nishi, H., Nomura, R., Norris, R. D., Pälike, H., Pares, J. M., Quintin, L., Raffi, I., Rea, B. R., Rea, D. K., Steiger, T. H., Tripati, A., Vandenberg, M. D. &. Wade, B. (2002): Paleogene equatorial transect: sites 1215-1222. – Proc. ODP, Init. Rep., **199** [http://www-odp.tamu.edu/publications/199_IR/199ir.htm].

MARTINI, E. (1971): Standard Tertiary and Quaternary calcareous nannoplankton zonation. – In: FARINACCI, A. (Ed.): Proceedings of the Second Planktonic Conference Roma 1970, Edizioni Tecnoscienza, Roma, **2**: 739-785.

MCFADDEN, P. L. & MCELHINNY, M. W. (1981): Classification of the reversal test in paleomagnetism. – Geophys. J. Int., **103**: 725-729.

MOLINA, E., COSOVIC, V., GONZALVO, C. & VON SALIS, K. (2000): Integrated biostratigraphy across the Ypresian/Lutetian boundary at Agost, Spain. – Rev. Micropaleontol., **43**: 381-391.

MONECHI, S. & THIERSTEIN, H. R. (1985): Late Cretaceous-Eocene nannofossil and magnetostratigraphic correlations near Gubbio, Italy. – Mar. Micropaleontol., **9**: 419-440.

NAPOLEONE, G., PREMOLI SILVA, I., HELLER, F., CHELI, P., COREZZI, S. & FISCHER, A. G. (1983: Eocene magnetic stratigraphy at Gubbio, Italy, and its implications for Paleogene geochronology. – Geol. Soc. Amer. Bull., **94**: 181-191.

OKADA, H. & BUKRY, D. (1980): Supplementary modification and introduction of code numbers to the low-latitude coccolith biostratigraphic zonation (BUKRY, 1973; 1975). – Mar. Micropal, **5**: 321-325.

ORUE-ETXEBARRIA, X. (1985): Descripción de dos nuevas especies de foraminíferos planctónicos en el Eoceno costero de la provincia de Bizkaia. – Rev. Esp. Micropaleontol., **17**: 467-477.

ORUE-ETXEBARRIA, X. & APELLANIZ, E. (1985): Estudio del límite Cuisiense-Luteciense en la costa vizcaína por medio de los foraminíferos planctónicos. – Newsl. Stratigr., **15**: 1-12.

ORUE-ETXEBARRIA, X. & LAMOLDA, M. (1985): Caractéristiques paléobiogéographiques du bassin Basco-Cantabrique pendant le Paléogène. – Rev. Micropaléontol., **27**: 257-265.

ORUE-ETXEBARRIA, X., LAMOLDA, M. & APELLANIZ, E. (1984): Bioestratigrafía del Eoceno Vizcaíno por medio de los foraminíferos planctónicos. – Rev. Esp. Micropaleontol., **16**: 241-263.

PAYROS, A. (1997): El Eoceno de la Cuenca de Pamplona: estratigrafía, facies y evolución paleogeográfica (Ph.D. thesis). – 403 pp.; Bilbao (Univ. of the Basque Country).

PAYROS, A., ORUE-ETXEBARRIA, X. & PUJALTE, V. (2006): Covarying sedimentary and biotic fluctuations in Lower-Middle Eocene Pyrenean deep-sea deposits: palaeoenvironmental implications. – Palaeogeogr., Palaeoclimatol., Palaeoecol., **234**: 258-276.

PERCH-NIELSEN, K. (1971): Elektronenmikroskopische Untersuchungen an Coccolithen und verwandten Formen aus dem Eoczän von Dänmark. – K. Dan. Vidensk. Selsk. Biol. Skr., **18**: 1-76.

– (1985): Cenozoic calcareous nannofossils. - In: BOLLI, H. M., SAUNDERS, J. B. & PERCH-NIELSEN, K. (Eds.): Plankton stratigraphy, p. 427-554; Cambridge (Cambridge Univ. Press).

PLAZIAT, J. C. (1981): Late Cretaceous to Late Eocene paleogeographic evolution of southwest Europe. – Palaeogeogr., Palaeoclimatol., Palaeoecol., **36**: 263-320.

PREMOLI SILVA, I. & BOERSMA, A. (1988): Atlantic planktonic foraminiferal historical biogeography and paleohydrographic indices. – Palaeogeogr., Palaeoclimatol., Palaeoecol., **67**: 315-356.

PREMOLI SILVA, I., RETTORI, R. & VERGA, D. (2003): Practical manual of Paleocene and Eocene planktonic foraminifera. – In: RETTORI, R. & VERGA, D. (Eds): International school on planktonic foraminifera, 2nd course, Paleocene and Eocene. – 152 pp.; Perugia (Univ. Perugia, Tipografia Pontefelcino).

PUJALTE, V., BACETA, J. I. & PAYROS, A. (2002): Tertiary: Western Pyrenees and Basque-Cantabrian region. – In: GIBBONS, W. & MORENO, T. (Eds.): The geology of Spain, p. 293-301; London (Geol. Society).

PUJALTE, V., PAYROS, A., ORUE-ETXEBARRIA, X. & BACETA, J. I. (1997). Secuencia evolutiva de los depósitos resedimentados eocenos de Punta Galea, Bizkaia: relevancia para determinación del sentido de transporte de láminas de "slump". – Geogaceta, **22**: 169-172.

PUJALTE, V., ROBLES, S., ORUE-ETXEBARRIA, X., BACETA, J. I., PAYROS, A. & LARRUZEA, I. F. (2000): Uppermost Cretaceous-Middle Eocene strata of the Basque-Cantabrian Region and western Pyrenees: a sequence stratigraphic perspective. – Rev. Soc. Geol. Esp., **13**: 191-211.

RAT, P. (1959) : Les pays Crétacés Basco-Cantabriques (Espagne) [Ph.D. thesis Univ. of Dijon]. – 525 pp; Dijon.

REMANE, J., BASSETT, M. G., COWIE, J. W., GOHRBANDT, K. H., LANE, R., MICHELSEN, O. & NAIWEN, W. (1996): Revised guidelines for the establishment of global chronostratigraphic standards by the International Commission on Stratigraphy. – Episodes, **19**: 77-81.

RODRÍGUEZ-LÁZARO, J. & GARCÍA-ZARRAGA, E. (1996): Paleogene deep-marine ostracodes from the Basque Basin. – In: Proc. 2nd European Ostracodologist Meeting, Glasgow 1993; Brit. Micropaleontol. Soc., p. 79-85.

ROMEIN, A. J. T. (1979): Lineages in early Paleogene calcareous nannoplankton. – Utrecht Micropalaeont. Bull., **22**: 1-230.

ROTH, P. H. & THIERSTEIN, H. (1972): Calcareous nannoplankton: leg 14 of the Deep Sea Drilling Projcet. – In: HAYES, D. E., PIMM, A. C., BECKMAN, J. P., BENSON, W. E., BERGER, W. H., ROTH, P. H., SUPKO, P. R. & VON RAD, V. (Eds.): Init. Rep. DSDP, **14**: 421-485.

SCHAUB, H. (1981): Nummulites et Assilines de la Tethys Paléogène: taxinomie, phylogénesè et biostratigraphie. – Mém. Suisses Paleontol., **104-106**: 236 pp.

SERRA-KIEL, J., HOTTINGER, L., CAUS, E., DROBNE, K., FERRANDEZ, C., JAUHRI, A. K., LESS, G., PAVLOVEC, R., PIGNATTI, J., SAMSO, J. M., SCHAUB, H., SIREL, E., STROUGO, A., TAMBAREAU, Y., TOSQUELLA, J. & ZAKREVSKAYA, E. (1998): Larger foraminiferal biostratigraphy of the Tethyan Paleocene and Eocene. – Bull. Soc. Geol. France, **169**: 281-299.

STAINFORTH, R. M., LAMB J. L., LUTERBACHER, H., BEARD, J. H. & JEFFORS, R. M. (1975): Cenozoic planktonic foraminifera zonation and characteristics of index forms. – Lawrence (Univ. of Kansas), Paleont. Contr., **62**: 1-425.

STEURBAUT, E. (1988): New Early and Middle Eocene calcareous nannoplankton events and correlations in middle to high latitudes of the northern hemisphere. – Newsl. Stratigr., **18**: 99-115.

TOSQUELLA, J. & SERRA-KIEL, J. (1996): Los nummulitidos (*Nummulites* y *Assilina*) del Paleoceno Superior-Eoceno Inferior de la Cuenca Pirenaica: Sistemática. – Acta Geol. Hisp., **31**: 37-159.

TOUMARKINE, M. & LUTERBACHER, H. (1985): Paleocene and Eocene planktonic foraminifera. – In: BOLLI, H. M., SAUNDERS, J. B. & PERCH-NIELSEN, K. (Eds): Plankton stratigraphy, p. 87-154; Cambridge (Cambridge Univ. Press).

TOWNSEND, H. A. & HAILWOOD, E. A. (1985): Magnetostratigraphic correlation of Palaeogene sediments in the Hampshire and London Basins, southern UK. – J. Geol. Soc., London, **142**: 957-982.

VAIL, P. R., AUDEMARD, F., BOWMAN, S. A., EISNER, P. N. & PEREZ-CRUZ, C. (1991): The stratigraphic signatures of tectonics, eustasy and sedimentology – An overview. – In: EINSELE, G., RICKEN, W. & SEILACHER, A. (Eds.): Cycles and events in stratigraphy, p. 617-659; Berlin (Springer).

VAROL, O. (1989): Eocene calcareous nannofossils from Sile, (Northwest Turkey). – Rev. Esp. Micropaleontol., **21**: 273-320.

VERGES, J., MILLÁN, H., ROCA, E., MUÑOZ, J. A., MARZO, M., CIRES, J., DEN BEZEMER, T., ZOETMELJER, R. & CLOETINGH, S. (1995): Eastern Pyrenees and related foreland basins: pre-, syn-, and post-collisional crustal-scale cross sections. – Mar. Petrol. Geol., **12**: 893-915.

ZACHOS, J. C., KROON, D., BLUM, P., BOWLES, J., GAILLOT, P., HASEGAWA, T., HATHORNE, E., HODELL, D. A., KELLY, D. C., JUNG, J. H., KELLER, S. M., LEE, Y. S., LEUSCHNER, D. C., LIU, Z., LOHMANN, K. C., LOURENS, L., MONECHI, S., NICOLO, M., RAFFI, I., RIESSELMAN, C., RÖHL, U., SCHELLEMBERG, S. A., SCHMIDT, D., SLUIJS, A., THOMAS, D., THOMAS, E. & VALLIUS, H. (2004): Early Cenozoic extrem climates: the Walvis Ridge transect. – Proc. ODP, Init. Rep., **208** [http://www-odp.tamu.edu/publications/208-IR/208ir.htm].

ZIJDERVELD, J. D. A. (1967): A.C. demagnetization of rock: analysis of results. – In: COLLINSON, D. W., CREER, K. M. & RUNCORN, S. K. (Eds.): Methods in paleomagnetism, p. 254-286; Amsterdam (Elsevier).

Manuscript received: March 28th, 2006.
Accepted by the Stuttgart editor: May 5th, 2006.

Addresses of the authors:

Dr. G. BERNOLA*, Dr. X. ORUE-ETXEBARRIA, Dr. A. PAYROS, Dr. E. APELLANIZ, F. CABALLERO, Departamento de Estratigrafía y Paleontología, Facultad de Ciencia y Tecnología, Universidad del País Vasco, Apdo. 644, E-48080 Bilbao;

Dr. J. DINARÈS-TURELL, Istituto Nazionale di Geofisica e Vulcanologia, Lab. Di Paleomagnetismo, Via di Vigna Murata, 605, I-00143 Rome;

Dr. J. TOSQUELLA, Departamento de Geodinámica y Paleontología, Facultad de Ciencias Experimentales, Universidad de Huelva, Campus del Carmen, Avenida de las Fuerzas Armadas s/n, E-21071 Huelva.

(*) Corresponding author: gilen.bernaola@ehu.es